Universidad de Concepción

Dirección de Postgrado

Facultad de Ciencias Físicas y Matemáticas - Doctorado Ciencias en Físicas

Asymptotically Anti-de Sitter Rotating Black Holes and Wormholes

Agujeros negros rotantes asintóticamente Anti-de Sitter y agujeros de gusano

Tesis para optar al grado de Doctora en Ciencias Físicas

Daniela Narbona Olivares

CONCEPCIÓN-CHILE

2024

Profesor Guía: Julio Oliva Zapata

Departamento de Física, Facultad de Ciencias Físicas y Matemáticas

Universidad de Concepción

Universidad de Concepción

Dirección de Postgrado

Facultad de Ciencias Físicas y Matemáticas - Doctorado en Ciencias Físicas

Anti-de Sitter Asymptotically Rotating Black Holes and Wormholes

Agujeros negros rotantes asintóticamente Anti-de Sitter y agujeros de gusano

Tesis para optar al grado de Doctora en Ciencias Físicas

DANIELA NARBONA OLIVARES

CONCEPCIÓN-CHILE

2024

Comisión evaluadora:

Dr. Octavio Fierro

Dr. Guillermo Rubilar

Agradecimientos

Me gustaría extender mi más profundo agradecimiento a mi esposo, Franco Olivares, por su apoyo incondicional durante este viaje. Su aliento, paciencia y fe inquebrantable han sido grandes fortalezas en este camino. Él ha estado a mi lado en cada desafío y su amor ha sido una fuente de motivación constante. También quiero agradecer a nuestra querida gatita Periquita, quien nos eligió como sus compañeros de vida. Su amor incondicional, felicidad y compañía han sido una fuente constante de alegría y consuelo, especialmente durante los momentos más exigentes de mi investigación.

Estoy profundamente agradecida a mi tutor de tesis, Julio Oliva, cuya guía, experiencia y paciencia han sido fundamentales para la realización de esta tesis. Sus valiosos comentarios, apoyo continuo y dedicación a mi crecimiento académico han sido invaluables. La tutoría de Julio no sólo ha enriquecido mi investigación, sino que también me ha ayudado a crecer como científica. Su capacidad para inspirarme y desafiarme ha sido crucial para afrontar las complejidades de mi trabajo. Gracias Julio por creer en mi potencial y por tu apoyo incondicional durante este viaje.

También quiero expresar mi agradecimiento al cuerpo docente y al personal de la Universidad de Concepción, particularmente a la Facultad de Ciencias Físicas y Matemáticas, por brindar un ambiente académico estimulante. Los recursos y el apoyo ofrecidos por la universidad han sido fundamentales en mi investigación.

Mi más sincero agradecimiento a mis hermanas Loreto y Sofía Narbona por su constante aliento y cariño. Su apoyo ha sido un pilar de fortaleza para mí y estoy profundamente agradecida por su presencia.

Contents

Agradecimientos **ii**

List of Figures **v**

Publications **vi**

Abstract **vii**

1 Introduction **2**

1.1 Description of the problems along with some historical background 2

1.2 Synopsis of the chapters 4

2 Preliminaries **6**

2.1 Einstein field equation 6

2.2 Some solutions of Einstein's equations 8

2.2.1 Anti-de Sitter spacetime 8

2.2.2 The BTZ Black Hole 8

2.3 Quasinormal and normal modes of scalars in BTZ, and AdS 10

3 Scalar probes on wormholes in Lovelock theories with unique vacuum **14**

3.1 Introduction 15

3.2 Embedding the wormhole in Lovelock theories in even dimensions 18

3.3 Normal modes of the scalar probe 19

3.4 Spectra for the minimally coupled scalar probe 23

3.5 Scalars probes with nonminimal coupling 25

3.6 Scalar Probe Dynamics in a Regularized Wormhole Spacetime 27

3.7 A new wormhole solution of Einstein-Gauss-Bonnet and Lovelock theories . 30

4 (Quasi)normal modes of de Sitter black holes and solitons in New Massive Gravity **33**

4.1 New Massive Gravity 34

4.2 Black hole 36

4.3 Gravitational soliton 39

5 Beyond static spacetimes **43**

5.1 Newman-Penrose formalism 44

5.2 Kerr-AdS black hole 46

5.3 Black Spindle 48

5.4 Axisymmetric modes in Black Spindle 50

5.5 Kerr AdS black holes in higher dimensions 51

5.6 Black Spindle in higher dimensions 52

5.7 Axisymmetric modes for higher dimensions 53

6 Conclusions **56**

Bibliography **62**

List of Figures

3.1 Effective potential for the radial dependence of the scalar probe, for different values of the parameters. As expected in the presence of a negative cosmological constant, the potential diverges at the boundaries $\bar{\rho} = 0, \pi$. . . 22

3.2 Spectra for the fundamental mode $p = 0$ (left-panel) and tenth overtone $p = 10$ (right-panel) as a function of ρ_0 for different even values of the angular momentum of the scalar probe $n = 0, 2, 4, ..., 10$, for $m^2 = 10$. The fundamental mode has a monotonic behavior with ρ_0 while excited frequencies present a maximum for a given critical value of ρ_0 which depends on the angular momentum of the field. 25

3.3 Spectra for vanishing angular momentum $n = 0$ (left-panel) and a spinning scalar probe with $n = 10$ (right-panel) as a function of ρ_0 for the fundamental mode and the first 10 excited states ($m^2 = 10$). 26

3.4 Fundamental and first two overtones for the scalar probe with $n = 0, 1, 2, 3, 4$, and $m^2 = 6$ (left-panel) and $m^2 = 30$ (right-panel). For a given value of ρ_0 the same frequency can be obtained for different modes since the effective potential depends explicitly on n. 27

3.5 Fundamental and first overtones for the nonminimally coupled scalar probe without angular momentum ($n = 0$, left), and $n = 10$ (right), for $m^2 = 10$ and $\xi = 3/8$. The figure in the left smoothly connects two fully resonant spectra for $\rho_0 = 0$ and $\rho_0 \to \infty$. 28

3.6 First three modes spectra for $\xi = 1/4$ (left) and $\xi = 3/8$ (right) for $m^2 = 10$ for $n = 0, 1, 2, 3, 4$. 28

Publications

The contents of Chapter 3 appear in the work (O. Fierro, D. Narbona, J. Oliva, C. Quijada, G. Rubilar,) published in Phisical Review D. The contents of Chapter 4 (D. Narbona) form part of a manuscript that is submitted for publication.

Abstract

This doctoral thesis explores advanced concepts in theoretical physics, focusing on asymptotically Anti-de Sitter (AdS) rotating black holes and wormholes within the framework of Lovelock theories and New Massive Gravity (NMG). The work is divided into several key problems:

- **Wormhole Construction in Lovelock Theories:** The thesis introduces new wormhole solutions in vacuum scenarios within Lovelock theories, particularly when coupling constants are aligned to create a unique vacuum. The study examines the effects of an integration constant on the energy content and stability of the wormholes, along with the spectrum of massive scalar probes.

- **Quasinormal Modes in NMG:** The research investigates scalar field perturbations over asymptotically de Sitter black holes and gravitational solitons within NMG, a three-dimensional theory that extends General Relativity. The work provides exact quasinormal modes, offering insights into the stability and dynamics of these spacetimes.

- **Rotating Black Holes:** The thesis delves into the perturbative dynamics of rotating black holes, particularly the Kerr-AdS black hole and the Black Spindle, which is obtained by applying the limit $a \to \ell$ to the Kerr-AdS black hole. Using the Newman-Penrose formalism and Teukolsky's master equation, the study analyzes the behavior of various fields under perturbations in rotating black hole spacetimes.

Overall, this thesis contributes to the understanding of complex gravitational phenomena, including the stability of wormholes and rotating black holes, and the implications of these solutions for higher-curvature gravity theories.

Resumen

Esta tesis doctoral explora conceptos avanzados en física teórica, enfocándose en agujeros negros rotantes asintóticamente Anti-de Sitter (AdS) y agujeros de gusano dentro del marco de las teorías de Lovelock y la Nueva Gravedad Masiva (NMG). El trabajo se divide en varios problemas clave:

- **Construcción de Agujeros de Gusano en Teorías de Lovelock:** La tesis introduce nuevas soluciones de agujeros de gusano en escenarios de vacío dentro de las teorías de Lovelock, particularmente cuando las constantes de acoplamiento están alineadas para crear un vacío único. El estudio examina los efectos de una constante de integración en el contenido energético y la estabilidad de los agujeros de gusano, junto con el espectro de campos escalares masivos.

- **Modos Cuasinormales en NMG:** La investigación investiga las perturbaciones de campos escalares en espaciotiempos de agujeros negros y solitones gravitacionales asintóticamente de Sitter tridimensionales dentro de NMG, una teoría tridimensional que extiende la Relatividad General. El trabajo proporciona modos cuasinormales exactos, ofreciendo ideas sobre la estabilidad y la dinámica de estos espaciotiempos.

- **Agujeros Negros Rotantes:** La tesis analiza la dinámica perturbativa de agujeros negros rotantes, en particular el agujero negro Kerr-AdS y el Black Spindle, que se obtiene aplicando el límite $a \to \ell$ al agujero negro Kerr-AdS. Usando el formalismo de Newman-Penrose y la ecuación maestra de Teukolsky, el estudio analiza el comportamiento de varios campos bajo perturbaciones en espaciotiempos de agujeros negros rotantes.

En conjunto, esta tesis contribuye a la comprensión de fenómenos gravitacionales complejos, incluyendo la estabilidad de los agujeros de gusano y los agujeros negros rotantes, y las implicaciones de estas soluciones para teorías de gravedad de curvatura elevada.

Chapter 1

Introduction

1.1 Description of the problems along with some historical background

Problem 1

Wormholes have fascinated physicists since the early 20th century when Ludwig Flamm first proposed the concept in 1916 as a solution to Einstein's field equations. However, it was John Wheeler who popularized the term "wormhole" in the 1950s. Lovelock theories, introduced by David Lovelock in 1971, generalize Einstein's General Relativity to higher dimensions while retaining second-order field equations. These theories incorporate higher-order curvature terms, offering richer gravitational dynamics and admitting new black holes and wormholes solutions.

The challenge in this problem is to construct new wormhole solutions in vacuum scenarios within Lovelock theories when the coupling constants are adjusted so that all solutions are maximally symmetric. This alignment creates a unique vacuum that simplifies the analysis but also introduces new complexities, such as the influence of an integration constant ρ_0 on the energy content and stability of the wormhole. The problem involves exploring the spectrum of massive, (non)minimally coupled scalar probes with Dirichlet boundary conditions, leading to a deformed Breitenlohner-Freedman bound sensitive to ρ_0.

Problem 2

The study of black holes and their perturbations has been a central topic in theoretical physics since the discovery of the Schwarzschild solution in 1916. Quasinormal modes (QNMs) were first explored in the 1950s to understand how perturbations evolve in black hole spacetimes, leading to insights into their stability and the emission of gravitational waves. New Massive Gravity (NMG) is a three-dimensional theory introduced by Bergshoeff, Hohm, and Townsend in 2009, extending Einstein's General Relativity by adding higher-order curvature terms to include massive gravitons while preserving unitarity.

In this problem we focus on studying the scalar field perturbations over asymptotically de Sitter (dS) three-dimensional black hole spacetimes and gravitational solitons in NMG. The challenge is to calculate the exact QNMs for these spacetimes, providing insights into their stability and the dynamics of perturbations. Understanding QNMs is crucial for interpreting gravitational wave signals and exploring the properties of black holes and solitons in higher-curvature gravity theories like NMG in dimension three.

Problem 3

The study of rotating black holes gained prominence with Roy Kerr's 1963 solution to Einstein's field equations, describing a rotating black hole. This Kerr solution marked a significant advance in astrophysics, as most stellar objects, including black holes, possess angular momentum. The Newman-Penrose formalism, developed in the 1960s, provided a powerful tool for analyzing spacetime geometries and field perturbations using spin coefficients. Teukolsky's master equation, derived in the 1970s, allowed for the separation of variables in the study of perturbations in rotating black holes, leading to significant progress in understanding their behavior.

Our problem here is to study the perturbative dynamics of rotating black holes, specifically the Kerr black hole, given their astrophysical relevance. Unlike static black holes, rotating black holes exhibit axial symmetry, complicating the analysis of perturbations. The challenge involves using the Newman-Penrose formalism and Teukolsky's master equation to study the behavior of various fields, such as scalar, electromagnetic, gravitational, and fermion fields, under perturbations in the spacetime of rotating black holes. This analysis is crucial for understanding the stability, resonance properties, and potential observational

signatures of rotating black holes.

These problems highlight the complexities and nuances in the study of advanced gravitational theories and their implications for our understanding of spacetime, black holes, and the fundamental forces of the Universe.

1.2 Synopsis of the chapters

Chapter 2 introduces the essential notation and conventions used throughout the thesis. It begins with Einstein's field equations, which assumes that the metric $g_{\mu\nu}$ of a Lorentzian spacetime in arbitrary holonomic coordinates x^μ is given by $ds^2 = g_{\mu\nu}dx^\mu dx^\nu$. The chapter discusses the geodesic equation, the Levi-Civita connection, and the curvature tensor (Riemann tensor). These foundational concepts in General Relativity are crucial for understanding the subsequent analysis of black holes and spacetime geometries.

Chapter 3 constructs new wormhole solutions within Lovelock theories in vacuum, particularly when coupling constants are such that all maximally symmetric solutions coincide. The wormholes are characterized by an integration constant ρ_0, influencing the energy content from one boundary. The study explores the effects of ρ_0 on the spectrum of massive, (non)minimally coupled scalar probes with Dirichlet boundary conditions. A deformed Breitenlohner-Freedman bound emerges, dependent on ρ_0. Detailed numerical analyses of the scalar spectra in five dimensions are provided, along with new wormhole geometries in the Einstein-Gauss-Bonnet theory with a unique vacuum.

Chapter 4 examines scalar field perturbations over asymptotically de Sitter (dS) three-dimensional black hole spacetimes and gravitational solitons in NMG. It introduces the hairy black hole solution of massive 3D gravity and analytically calculates the exact quasinormal modes (QNMs) of scalar perturbations for the hairy black hole. The chapter also explores the asymptotically dS_3 soliton, calculating the normal modes (NMs) exactly. This comprehensive analysis contributes to understanding the stability and dynamics of these novel black hole and soliton solutions under scalar field perturbations.

Chapter 5 focuses on rotating black holes, given the astrophysical significance of stellar rotation. It discusses the limitations of the Regge-Wheeler method for rotating Kerr black holes and introduces the Newman-Penrose formalism, which, combined with Petrov type D spacetimes, leads to Teukolsky's master equation. This equation is crucial for

studying the perturbations of scalar, electromagnetic, gravitational, and fermion fields in rotating black hole spacetimes. The chapter delves into the behavior of these fields under perturbations, emphasizing the necessity of these studies for understanding the complexities of rotating black holes.

These chapters collectively lay a robust foundation for exploring advanced topics in General Relativity, black hole physics, and the dynamics of various fields in curved spacetimes.

Chapter 2

Preliminaries

In this chapter, we will introduce the notation and conventions that will be used in the following chapters. To deepen into the contents of General Relativity, one can see (1), and to study black holes in greater detail one can see for example (2).

2.1 Einstein field equation

General Relativity assumes that the metric $g_{\mu\nu}$ of a Lorentzian spacetime, in arbitrary holonomic coordinates x^μ, is given by

$$ds^2 = g_{\mu\nu}dx^\mu dx^\nu, \tag{2.1.1}$$

where for a spacetime in 4 dimensions $\mu, \nu = 0, 1, 2, 3$ and we will be using the Lorentz signature $(-, +, +, +)$. Having adequately defined the Riemannian metric, the geodesic equation for it takes the following form

$$\frac{d^2x^\mu}{d\tau^2} + \Gamma^\mu_{\nu\lambda}\frac{dx^\nu}{d\tau}\frac{dx^\lambda}{d\tau} = 0, \tag{2.1.2}$$

where τ is the proper time and $\Gamma^\mu_{\nu\lambda}$ are the Levi-Civita connection, or Christoffel symbols for the metric (2.1.1), which are given by

$$\Gamma^\mu_{\nu\lambda} = \frac{1}{2}g^{\mu\alpha}(\partial_\nu g_{\lambda\alpha} + \partial_\lambda g_{\alpha\nu} - \partial_\alpha g_{\nu\lambda}). \tag{2.1.3}$$

This is the unique torsionless connection compatible with the metric (2.1.1). The

Christoffel symbols allow us to introduce the curvature tensor, also called the Riemann tensor, which is given by

$$R^{\mu}{}_{\nu\rho\sigma} = \partial_\rho \Gamma^{\mu}{}_{\nu\sigma} - \partial_\sigma \Gamma^{\mu}{}_{\nu\rho} + \Gamma^{\mu}{}_{\alpha\rho}\Gamma^{\alpha}{}_{\nu\sigma} - \Gamma^{\mu}{}_{\alpha\sigma}\Gamma^{\alpha}{}_{\nu\rho}. \tag{2.1.4}$$

From this definition, we can see that the Riemann curvature satisfies the following antisymmetric property

$$R^{\mu}{}_{\nu\rho\sigma} \equiv -R^{\mu}{}_{\nu\sigma\rho}. \tag{2.1.5}$$

Now, if we consider the totally covariant components of the curvature tensor, $R_{\mu\nu\rho\sigma} := g_{\mu\alpha}R^{\alpha}{}_{\nu\rho\sigma}$, for a Riemannian geometry, that is, when the connection is the Christoffel symbol of the metric, the Riemann curvature tensor has the following antisymmetries

$$R_{\mu\nu\rho\sigma} = -R_{\nu\mu\rho\sigma}, \tag{2.1.6}$$

$$R_{\mu\nu\rho\sigma} = R_{\rho\sigma\mu\nu}, \tag{2.1.7}$$

and also

$$R_{\mu\nu\rho\sigma} + R_{\mu\rho\sigma\nu} + R_{\mu\sigma\nu\rho} = 0 \qquad \Leftrightarrow \qquad R_{\mu[\nu\rho\sigma]} = 0. \tag{2.1.8}$$

From the Riemann tensor, we can define the Ricci tensor

$$R_{\rho\sigma} = R^{\mu}{}_{\rho\mu\sigma}, \tag{2.1.9}$$

which, in a space with Riemannian geometry, is symmetric $R_{\rho\sigma} = R_{\sigma\rho}$. Furthermore, we can define the Ricci scalar, as follows

$$R = g^{\mu\nu}R_{\mu\nu}. \tag{2.1.10}$$

Now we have all the tools to introduce Einstein's field equations. With G as Newton's gravitational constant and c as the speed of light in vacuum, we define Einstein's gravitational constant $\kappa := 8\pi G/c^4$. So, Einstein's field equations with cosmological constant Λ read

$$R_{\mu\nu} - \frac{1}{2}g_{\mu\nu}R + \Lambda g_{\mu\nu} = \kappa T_{\mu\nu}, \tag{2.1.11}$$

where the right hand side of this equation is the source represented by the energy-momentum tensor $T_{\mu\nu}$.

2.2 Some solutions of Einstein's equations

2.2.1 Anti-de Sitter spacetime

Anti-de Sitter (AdS) spacetime is the maximally symmetric solution of Einstein's equations in a vacuum with a negative cosmological constant, and therefore it has negative constant curvature. In this way, the AdS spacetime is not useful to describe the late accelerated expansion of our Universe, since the observed cosmological constant of our Universe is positive $\Lambda \sim 10^{-52}\,\mathrm{m}^{-2}$ (3).

However, when Maldacena established the AdS-CFT conjecture in 1998 (4), the AdS spacetime became a very interesting area for the high-energy physics community. The main features of this conjecture are that there is a holographic mapping between a quantum theory of gravity (string theory) and an ordinary non-gravitational quantum field theory (CFT), where the AdS spacetime has one more spatial dimension than the spacetime where the CFT lives on, and that AdS-CFT is a strong/weak coupling duality, i.e. in cases where the gauge theory of the interactions are intense and complex to explore, it corresponds to a string theory with weaker interactions.

The D-dimensional AdS spacetime in static global coordinates also called Schwarzschild coordinates is given by

$$ds^2 = -\left(1 + \frac{r^2}{\ell^2}\right) dt^2 + \frac{dr^2}{1 + \frac{r^2}{\ell^2}} + r^2 d\Omega_p^2, \tag{2.2.1}$$

where $r \geq 0$, $p = D - 2$, $d\Omega_p^2$ is the $p-$sphere metric, ℓ is called the length or AdS radius, and is related to the cosmological constant by $\Lambda = -(D-1)(D-2)/2\ell^2$.

2.2.2 The BTZ Black Hole

Bañados, Teitelboim, and Zanelli (BTZ) (5), showed in 1992 that $(2+1)$-dimensional gravity has a black hole solution. The BTZ black hole has well-defined charges at infinity, such as mass and angular momentum. In fact, a rotating BTZ black hole has an inner and outer horizon, analogous to the Kerr black hole. Furthermore, as this black hole is

asymptotically AdS, one can study the implications of the AdS-CFT conjecture, specifically the AdS-CFT duality, which gives a prediction for the timescale of the dual CFT thermalization (4).

The BTZ black hole can be described by the following metric

$$ds^2 = -N^2 dt^2 + N^{-2} dr^2 + r^2 (N^\varphi dt + d\varphi)^2, \tag{2.2.2}$$

where the squared lapse $N^2(r)$ and the angular shift $N^\varphi(r)$ functions are given by

$$N^2(r) = -M + \frac{r^2}{\ell^2} + \frac{J^2}{4r^2}, \quad N^\varphi(r) = -\frac{J}{2r^2}, \tag{2.2.3}$$

with $-\infty < t < \infty$, $0 < r < \infty$ and $0 \leq \varphi \leq 2\pi$. The integration constants M and J represent the mass and angular momentum, respectively.

There are coordinate singularities at $r = r_\pm$, that is, the function $N^2(r)$ vanishes for two values of r given by

$$r_\pm = \ell \left[\frac{M}{2} \left(1 \pm \sqrt{1 - \left(\frac{J}{M\ell} \right)^2} \right) \right]^{1/2}, \tag{2.2.4}$$

which leads to:

$$M = \frac{r_+^2 + r_-^2}{\ell^2}, \quad J = \frac{2 r_+ r_-}{\ell}. \tag{2.2.5}$$

In this case, r_+ is the event horizon of this black hole. Note that for the event horizon to exist, the following inequality must hold

$$M > 0, \quad |J| \leq M\ell, \tag{2.2.6}$$

and in the extreme case $|J| = M\ell$, both roots of $N^2 = 0$ coincide, leading to the extremal BTZ black hole.

We can compare the AdS spacetime and the BTZ black hole. AdS is a regular spacetime, while the BTZ black hole has a singularity hidden by an event horizon and the outer region is asymptotically AdS.

On the other hand, the ergosurface is found by calculating the point where the time-time

component g_{00} of the metric vanishes. This occurs when $r = r_{erg}$, with

$$r_{erg} = M^{1/2}\ell = \left(r_+^2 + r_-^2\right)^{1/2}. \tag{2.2.7}$$

In the same way as the Kerr solution in 3+1 dimensions, the region where $r < r_{\text{erg}}$ defines an ergosphere: the timelike curves within this area must have $d\varphi/d\tau > 0$ (when $J > 0$), meaning all observers are dragged along by the black hole's rotation. Note that $r_\pm$ becomes complex if $|J| > M\ell$, causing the horizons to vanish and leaving a metric with a naked conical singularity at $r = 0$. The metric for $M = -1$, $J = 0$ can be recognized as that of ordinary anti-de Sitter space; it is separated by a mass gap from the "massless black hole" with $M = 0$, $J = 0$.

2.3 Quasinormal and normal modes of scalars in BTZ, and AdS

As in electromagnetism, one manner of characterizing a gravitational field is by studying probes like geodesics or field propagation on it, with scalar fields offering a particularly powerful tool. Represented by a single value at each point in space and time, scalar fields provide a simplified yet insightful way to probe gravitational properties. Their interaction with the gravitational field reveals crucial information about spacetime geometry, including curvature and gravitational lensing phenomena, and offers insights into the stability of configurations like black holes and wormholes. This approach, valuable in theoretical physics where exact gravitational solutions are hard to obtain, parallels the study of electromagnetic waves in understanding electromagnetism, enriching our comprehension of gravity by exploring spacetime intricacies and fundamental gravitational principles.

Scalar perturbations of AdS spacetime

We will study a scalar field with mass φ, given by the Klein-Gordon equation

$$\left(\Box - m^2\right)\varphi = 0, \tag{2.3.1}$$

where

$$\Box\varphi = \frac{1}{\sqrt{-g}}\partial_\mu\left(\sqrt{-g}g^{\mu\nu}\partial_\nu\right)\varphi, \tag{2.3.2}$$

and g is the determinant of the metric. Using the metric (2.2.1) with $d = 4$ we have that

$$\begin{aligned}\Box\varphi - m^2\varphi = &-\left(1+\frac{r^2}{\ell^2}\right)^{-1}\partial_t^2\varphi + \frac{2}{r}\left(1+2\frac{r^2}{\ell^2}\right)\partial_r\varphi + \left(1+\frac{r^2}{\ell^2}\right)\partial_r^2\varphi \\ &+\frac{1}{r^2}\frac{\cos(\theta)}{\sin(\theta)}\partial_\theta\varphi + \frac{1}{r^2}\partial_\theta^2\varphi + \frac{1}{r^2\sin^2(\theta)}\partial_\varphi^2\varphi - m^2\varphi \;=\; 0.\end{aligned} \tag{2.3.3}$$

We consider a separable solution of the form

$$\varphi(t, r, \theta, \phi) = T(t)R(r)Y(\theta, \phi), \tag{2.3.4}$$

we substitute in (2.3.3), rearrange terms, introduce the separation constants λ and ω and $\ell = 0$, obtaining the following set of differential equations

$$\frac{d^2T(t)}{dt^2} + \omega^2 T(t) = 0, \tag{2.3.5}$$

$$\nabla_{S^2}Y(\theta, \phi) + \lambda Y(\theta, \phi) = 0, \tag{2.3.6}$$

$$r^2\left(1+r^2\right)\frac{d^2R(r)}{dr^2} + 2r\left(1+2r^2\right)\frac{dR(r)}{dr} + \left(\frac{r^2\omega^2}{1+r^2} - m^2r^2 - \lambda\right)R(r) = 0. \tag{2.3.7}$$

Equation (2.3.5) is a harmonic oscillator equation whose solution is given by

$$T(t) = \alpha\cos(\omega t + \beta) \tag{2.3.8}$$

where α and β are integration constants.

On the other hand, equation (2.3.6) is an eigenvalue equation, where the eigenfunction is Y and the eigenvalue is $-\lambda$. Asking for regularity at the poles and for the function to be univalued for the angle ϕ, we obtain that the eigenvalues of the equation are given by $-\lambda = -l(l+1)$ with $l \in \mathbb{N}_0$ so that the eigenfunctions Y are the spherical harmonic functions $Y_{l,n}$ where $n = -l, \ldots 0, \ldots, l$.

Equation (2.3.7) is a hypergeometric differential equation, whose solution is of the form (6)

$$R(r) \;=\; \left(1+r^2\right)^{\frac{\omega}{2}}\left[C_1 r^l {}_2F_1\left(a, b; c; -r^2\right)\right.$$

$$+C_2 r^{-l-1}{}_2F_1\left(1+a-c, 1+b-c; 2-c; -r^2\right)\Big], \tag{2.3.9}$$

where

$$a = \frac{1}{2}\omega + \frac{3}{4} + \frac{1}{2}l + \frac{1}{4}\sqrt{4m^2+9}, \tag{2.3.10}$$

$$b = \frac{1}{2}\omega + \frac{3}{4} + \frac{1}{2}l - \frac{1}{4}\sqrt{4m^2+9}, \tag{2.3.11}$$

$$c = \frac{3}{2} + l, \tag{2.3.12}$$

and with $C_{1,2}$ constants of integration (remember that m is dimensionless at this point since we are in natural units and have defined $\ell = 1$). Imposing the regularity condition at the origin, we have that $C_2 = 0$, so that

$$R(r) = C_1\left(1+r^2\right)^{\frac{\omega}{2}} r^l {}_2F_1\left(a, b; c; -r^2\right). \tag{2.3.13}$$

Using properties of the hypergeometric functions we can rewrite

$$\begin{aligned} R(r) = C_1\left(1+r^2\right)^{\frac{\omega}{2}} r^l \Bigg[&\frac{\Gamma(c)\Gamma(b-a)}{\Gamma(c-a)\Gamma(b)}\left(\frac{1}{1+r^2}\right)^a {}_2F_1\left(a, c-b; a-b+1; \frac{1}{1+r^2}\right) \\ &+\frac{\Gamma(c)\Gamma(a-b)}{\Gamma(a)\Gamma(c-b)}\left(\frac{1}{1+r^2}\right)^b {}_2F_1\left(c-a, b; 1-a+b; \frac{1}{1+r^2}\right)\Bigg] \end{aligned} \tag{2.3.14}$$

Assuming that the function R vanishes at infinity, we obtain the condition $c - b = -j$, with $j \in \mathbb{N}_0$. This condition determines the field oscillation frequency spectrum, which is given by:

$$\omega = 2j + l + \frac{3}{2} + \sqrt{m^2 + \frac{9}{4}}, \tag{2.3.15}$$

with l and $j \in \mathbb{N}_0$.

Scalar perturbations of BTZ black hole

Cardoso and Lemos in 2001 (7) studied perturbations of different fields on the BTZ black hole (2.2.2) with $J = 0$ and $M = r_+^2/\ell^2$, including the scalar field. We begin by introducing a minimally coupled scalar field, whose equation is given by

$$\Box\Phi = 0, \tag{2.3.16}$$

and using the separation ansatz

$$\Phi = \frac{1}{r^{1/2}} f(r) e^{-i\omega t} e^{im\varphi}, \tag{2.3.17}$$

where m is the angular quantum number. The differential equation for the radial dependence is given by

$$\frac{d^2 f(r)}{dr_*^2} + (\omega^2 - V(r)) f(r) = 0, \tag{2.3.18}$$

where

$$V(r) = \frac{3r^2}{4\ell^4} - \frac{M}{2\ell^2} - \frac{M^2}{4r^2} + \frac{m^2}{\ell^2} - \frac{Mm^2}{r^2}, \tag{2.3.19}$$

and the tortoise coordinate r_* has been introduced, which in this case is defined from $dr_* = dr/(-M + r^2/\ell^2)$, and, therefore, is defined by $r = -\ell M^{1/2} \tanh(M^{1/2} r_*/\ell)$.

After a change of variable and a redefinition of the function $f(r)$, the equation (2.3.18) becomes the hypergeometric equation and satisfies the boundary conditions of ingoing waves near the event horizon and null at infinity. Thus equation (2.3.18) leads to an exact expression for the quasinormal frequency, given by (7)

$$\omega\ell = \pm m - 2i\frac{r_+}{\ell}(n+1), \tag{2.3.20}$$

with $n = 0, 1, 2, \ldots$ and, where the lowest frequencies ($n = 0$ and $m = 0$) correspond to the one already found in the same year by Govindarajan and Suneeta (8).

In (9) it was shown that Einstein-Gauss-Bonnet gravity admits smooth spacetimes connecting two asymptotically AdS geometries, i.e. wormholes. Therefore, the problem of explaining the scalar probes on such general spacetimes is natural. The next chapter presents such an explanation, that requires numerical tools and represents the first original result of this thesis.

In Chapter 4 we will give details of this type of computation for a novel black hole with a cosmological horizon.

Chapter 3

Scalar probes on wormholes in Lovelock theories with unique vacuum

In this chapter we construct new wormhole solutions of Lovelock theories in vacuum, when the coupling constants are such that all the maximally symmetric solutions coincide, extending wormhole solutions previously known in the Chern-Simons case to arbitrary dimensions. Like the latter, the wormholes are characterized by an integration constant ρ_0 that controls the contribution to the energy content from one of the boundaries. Then, we study the effects of the constant ρ_0 on the spectrum of a massive, (non)minimally coupled scalar probe, with Dirichlet boundary conditions at both asymptotic regions. As a result, a deformed Breitenlohner-Freedman bound emerges, which is sensitive to the value of ρ_0. The scalar spectra are numerically obtained in detail in dimension five, and in such dimension we also present a new family of wormhole geometries for the Einstein-Gauss-Bonnet theory with a unique vacuum. The new geometries are constructed via a double analytic continuation of a wormhole previously reported in the literature, but now the constant ρ_0 appears in the centrifugal terms of the equations for the geodesic and scalar probes. The mass of these configurations vanishes nontrivially, since the contributions to the mass integral from each boundary are nonvanishing, but only differ in sign, providing a new example of a spacetime having "mass without mass".

3.1 Introduction

In the realm of four dimensional General Relativity (GR), it is a difficult task to construct asymptotically flat, spherically symmetric wormhole geometries since they generally require violations of different energy conditions (10). In particular the averaged null energy condition must be circumvented for a wormhole to exist if the throat is to provide a shorter path connecting points of each asymptotic region through the bulk. The obstructions can be avoided, for instance, by going beyond GR (see, e.g., (11), (12) and references therein), by the inclusion of a NUT charge (13), or by constructing wormholes with long throats supported by Casimir energy (14). The inclusion of a negative cosmological constant allowed to construct asymptotically AdS wormholes which in the radial direction are foliated by warped AdS spacetimes and are devoid of closed timelike curves (15), which possess a noncontratible S^1, and contain a family of BPS configurations (16), these configurations are stable because they cannot evolve to lower energy configurations since there are no lower energy configurations..

The general features that a static metric must fulfill in order to describe a traversable, asymptotically flat wormhole were studied in the seminal papers (17), (18), and (19), and the metrics considered in such references have been used as toy models to study the propagation of probe fields on spacetimes with wormhole topology. For example, the propagation of scalar and electromagnetic waves may correctly lead to the interpretation of the wormhole geometry as an extended article (20). Transmission and reflection coefficients for asymptotically flat, ultrastatic wormholes in 2+1 and 3+1 dimensions have been studied in Refs. (21), (22), and (23), featuring resonances for particular values of the wormhole parameters, and leading to almost reflectionless effective potentials[1]. In Ref. (23) it was also shown that a nonminimally coupled scalar field may lead to an instability since the effective Schrödinger potential for the perturbation turns out to be negative definite. Even more, when the wormhole is asymptotically flat in both asymptotic regions, outgoing boundary conditions at both infinities lead to a quasinormal spectrum which can mimic that of a black hole of mass M for a given wormhole mass M^{-1} (23) (see also the recent works (28; 29) and references therein). By imposing boundary conditions on the

[1]There is also an extensive literature on Euclidean wormholes (see, e.g., (24)) leading to instantons and on the use of scalar probes to test the stability of the configuration (see, e.g., (25), (26) and references therein). It has been recently established that geometries with such properties can be embedded in M-theory (27). In this chapter, we will be interested in traversable, Lorentzian wormholes.

asymptotic AdS boundary as well as at the throat, a particular family of smooth wormholes in Einstein's theory coupled to a nonlinear electrodynamics has also been shown to be stable provided an effective Breitenlohner-Freedman bound (30; 31; 32) is fulfilled for the probe scalar field (33).

Asymptotically AdS wormholes in theories with quadratic terms in the curvature do exist in five dimensions (9), in vacuum. The action for the Einstein-Gauss-Bonnet theory in five dimensions reads

$$I = \frac{1}{16\pi G}\int \sqrt{-g}\left(R - 2\Lambda + \alpha\left(R^2 - 4R_{\mu\nu}R^{\mu\nu} + R_{\alpha\beta\gamma\delta}R^{\alpha\beta\gamma\delta}\right)\right)d^5x, \tag{3.1.1}$$

where α is a coupling constant with mass dimension equal to -2. When formulated in first order, the local Lorentz invariance of the theory is enlarged to a local (A)dS group at the point $\Lambda\alpha = -3/4$ (see, e.g., (34) and references therein). In this case, the Lagrangian can be written as a Chern-Simons form where the spin connection as well as the vielbein transform as components of an (A)dS gauge connection. This structure can be extended to higher odd-dimensions as well as to dimension three, but in contrast to the latter, the higher dimensional case does describe a theory with local degrees of freedom in the bulk. As shown in (5), all these theories contain generalizations of the static $2+1$-dimensional BTZ black hole (35)-(36), characterized by an integration constant which can be identified with the mass. In (9) it was shown that this theory actually admits a larger family of static solutions, including wormhole geometries in vacuum with two asymptotically locally AdS_{2n+1} regions for $n \geq 2$. In five dimensions, the line element of these solutions is given by

$$ds^2 = l^2\left[-\cosh^2(\rho-\rho_0)\,dt^2 + d\rho^2 + \cosh^2\rho\left(d\varphi^2 + d\Sigma_2^2\right)\right], \tag{3.1.2}$$

where $-\infty < t < \infty$, $-\infty < \rho < \infty$, $0 \leq \varphi < 2\pi$, identified, and $d\Sigma_2$ stands for the line-element of an Euclidean 2-dimensional manifold, whose local geometry is that of the hyperbolic space with radius $3^{-1/2}$, globally equivalent to the quotient of the hyperbolic space by a Fuchsian group, i.e., Σ_2 is homeomorphic to the quotient of H_2 by a freely acting, discrete subgroup of $SO(2,1)$. For any local purpose one can consider complex projective coordinates such that

$$d\Sigma_2^2 = \frac{1}{3}\left(1 - \frac{z\bar{z}}{4}\right)^{-2} dz d\bar{z}. \tag{3.1.3}$$

The spacetime (3.1.2) represents a wormhole geometry with a throat located at $\rho = 0$, connecting two asymptotically locally AdS spacetimes with curvature radius $l^2 = 4\alpha = -3/\Lambda$. The constant ρ_0 is an arbitrary integration constant and determines the apparent mass of the wormhole as seen by an asymptotic observer at a given asymptotic region (9)-(37). The presence of $\rho_0 \neq 0$, creates a region which has interesting properties for particles with angular momentum, probing these geometries. As shown in (37), the effective potential for the geodesics has two contributions, one of which is due to the angular momentum of the particle around the S^1 factor parametrized by the coordinate φ in (3.1.2). This centrifugal contribution always points outward the throat located at $\rho = 0$, while the remaining contribution flips its direction at the surface $\rho = \rho_0$ and always points toward it. Therefore, the gravitational pull acting on a particle can be balanced by the centrifugal contribution only if the particle is in one of the regions $-\infty < \rho < 0$ or $\rho_0 < \rho < +\infty$, for positive ρ_0. Geodesic probes turn out to be expelled from the region $0 < \rho < \rho_0$. And for probe strings propagating in this background the surface $\rho = \rho_0/2$ defines the turning point of strings with both ends attached to the same asymptotic region (38).

In arbitrary odd dimensions, $d = 2n + 1$, these wormholes can be embedded in Lovelock theories at the Chern-Simons point, at which the Lagrangian can be written as a Chern-Simons form for the $SO(2n, 2)$ group. In this chapter, first, we show that in even dimension, $d = 2n$, the wormhole geometry can also be embedded in Lovelock theory with a unique vacuum, when the maximum power in the curvature is present. Therefore we would have identified a sensible gravity theory in every dimension for which the wormhole geometry is a solution. Then we will study a minimally coupled massive scalar field on the wormhole geometry (3.1.2), revisiting the case with $\rho_0 = 0$ which can be solved analytically (see (39)). Following a complementary approach to that in Ref. (39), by formulating the problem in a Schrödinger form, we show that the effective potential for the scalar probe corresponds to a Rosen-Morse potential, which explains the integrability of the spectrum (40). Remarkably, we find that also in the limit $\rho_0 \to \infty$ the spectrum can be obtained in a closed form as well, which would be particularly useful for obtaining the normal frequencies of the scalar on wormholes with large ρ_0. Then, we will numerically solve the spectrum for normal frequencies of the scalar field for finite, nonvanishing values of ρ_0 in dimension five, connecting the two exactly solvable models. We also show that

there is an effective Breitenlohner-Freedman mass for the scalar probe, which depends on ρ_0. In the last section of this chapter, via a double Wick rotation, we construct a new family of wormholes, which maintain the properties of the asymptotic regions. We also show that the propagation of a scalar probe on the new family of wormholes, is equivalent to the propagation on the former geometries, by performing the double Wick rotation at the level of the quantum numbers, namely by setting $\omega \to in$ and $n \to i\omega$. Finally we obtain the mass of this new wormhole geometry.

3.2 Embedding the wormhole in Lovelock theories in even dimensions

Before analysing the propagation of a scalar probe on the wormhole geometry in arbitrary dimensions, below we identify a Lovelock theory which admits the wormhole as a vacuum solution, in even dimension. As mentioned before, in odd dimensions it is enough to consider Lovelock theory with the couplings related in such a manner that the action can be written as a Chern-Simons form for the AdS group. Since Lovelock theories with generic couplings fulfill a Birkhoff theorem (see (41; 42)), we will have to consider some relation between the couplings in order to by-pass such uniqueness result. For concreteness, let us focus on the Lovelock theory that has a unique maximally symmetric solution and contains all the possible powers of the curvature allowed in dimension d, i.e., we consider all the Lovelock terms of the form $\mathcal{R}^k$ with $k \leq [(d-1)/2]$. The field equations of such theory can be written in a very compact manner

$$E_B^A := \delta^{AC_1...C_{2k}}_{BD_1...D_{2k}} \bar{R}^{D_1D_2}_{C_1C_2} ... \bar{R}^{D_{2k-1}D_{2k}}_{C_{2k-1}C_{2k}} = 0 \ , \tag{3.2.1}$$

where $\bar{R}^{D_1D_2}_{C_1C_2} := R^{D_1D_2}_{C_1C_2} + l^{-2}\delta^{D_1D_2}_{C_1C_2}$. Here l is the curvature radius of the unique, maximally symmetric, AdS solution of the theory. Notice that all allowed powers of the curvature appear in the field equations. It is easy to see that for the wormhole geometry

$$ds^2 = l^2 \left[-\cosh^2(\rho - \rho_0)\, dt^2 + d\rho^2 + \cosh^2\rho d\Sigma^2_{d-2} \right] \ , \tag{3.2.2}$$

the components of the shifted curvature $\bar{R}^{AB}_{CD}$ are

$$\bar{R}^{t\rho}{}_{t\rho} = \bar{R}^{\rho i}{}_{\rho j} = 0,\ \bar{R}^{ti}{}_{tj} = \frac{(1-\tanh\rho\tanh(\rho-\rho_0))}{l^2}\delta^i_j\ , \tag{3.2.3}$$

$$\bar{R}^{ij}{}_{kl} = \tilde{R}^{ij}{}_{kl} + \delta^{ij}_{kl}\ , \tag{3.2.4}$$

where Latin indices $\{i,j,k,l\}$ are coordinate indices on the manifold Σ_{d-2}, which has an intrinsic Riemann tensor $\tilde{R}^{ij}{}_{kl}$. As explained in (9), in odd dimension $d = 2k+1$ the field equations imply a single scalar constraint on the Euclidean manifold Σ_{d-2},

$$\delta^{i_1\ldots i_{2k-2}}_{j_1\ldots j_{2k-2}}\left(\tilde{R}^{j_1j_2}{}_{i_1i_2} + \delta^{j_1j_2}_{i_1i_2}\right)\ldots\left(\tilde{R}^{j_{2k-3}j_{2k-2}}{}_{i_{2k-3}i_{2k-2}} + \delta^{j_{2k-3}j_{2k-2}}_{i_{2k-3}i_{2k-2}}\right) = 0\ , \tag{3.2.5}$$

which is solved for example by the manifold $S^1\times H_{d-3}$, with H_{d-3} with a suitable radius.

Here we are interested in the embedding of the wormhole geometry in a Lovelock theory with unique vacuum, in even dimension with $d = 2k+2$. In this case the field equations (3.2.1) reduce to a tensor and a scalar constraint on the manifold Σ_{d-2}, which respectively read

$$\delta^{ki_1\ldots i_{2k}}_{lj_1\ldots j_{2k}}\left(\tilde{R}^{j_1j_2}{}_{i_1i_2} + \delta^{j_1j_2}_{i_1i_2}\right)\ldots\left(\tilde{R}^{j_{2k-3}j_{2k-2}}{}_{i_{2k-3}i_{2k-2}} + \delta^{j_{2k-3}j_{2k-2}}_{i_{2k-3}i_{2k-2}}\right) = 0\ , \tag{3.2.6}$$

$$\delta^{i_1\ldots i_{2k}}_{j_1\ldots j_{2k}}\left(\tilde{R}^{j_1j_2}{}_{i_1i_2} + \delta^{j_1j_2}_{i_1i_2}\right)\ldots\left(\tilde{R}^{j_{2k-1}j_{2k}}{}_{i_{2k-1}i_{2k}} + \delta^{j_{2k-1}j_{2k}}_{i_{2k-1}i_{2k}}\right) = 0\ . \tag{3.2.7}$$

To fix ideas, if one considers these constraints in dimension six, they respectively reduce to that of an Einstein manifold with $\tilde{R}^i{}_j = -3\delta^i_j$ and a constant Kretchman scalar $\tilde{R}_{ijkl}\tilde{R}^{ijkl} = 36$. In consequence, provided we fulfill these conditions, we would have found a new wormhole solution of Lovelock theory with a unique vacuum in even dimensions. A simple inspection of these equations show that one can solve them by considering suitable products of constant curvature spacetimes, or even products of homogeneous geometries (see (43; 44)).

3.3 Normal modes of the scalar probe

The scalar probe

$$\left(\Box - m^2\right)\Phi(x^\mu) = 0\ , \tag{3.3.1}$$

on the wormhole geometry

$$ds^2 = l^2 \left[-\cosh^2(\rho - \rho_0)\, dt^2 + d\rho^2 + \cosh^2\rho \left(d\varphi^2 + d\Sigma_{d-3}^2 \right) \right], \tag{3.3.2}$$

can be separated as

$$\Phi(x) = \mathcal{R} \left(\sum_{n=-\infty}^{\infty} \int d\omega \; R_{\omega,n}(\rho) \; e^{-i\omega t + in\varphi} \right) , \tag{3.3.3}$$

and hereafter we will drop the dependence of $R_{\omega,n}(\rho)$ on ω and n. Notice that we have assumed the scalar probe to be independent of the coordinates parametrizing the manifold Σ_{d-3}. Since the equation is linear, one finds decoupled, second order, linear ODEs for each mode, leading to

$$\begin{aligned} 0 = {} & \partial_\rho \left[\cosh(\rho - \rho_0) \cosh^{d-2}(\rho) \partial_\rho R(\rho) \right] + \\ & + \cosh(\rho - \rho_0) \cosh^{d-2}(\rho) \left[\frac{\omega^2}{\cosh^2(\rho - \rho_0)} - \frac{n^2}{\cosh^2(\rho - \rho_0)} - m^2 l^2 \right] R(\rho). \end{aligned} \tag{3.3.4}$$

Had we considered dependence on the coordinates of Σ_{d-3}, by including in (3.3.3) an eigenfunction of the Laplace operator on Σ_{d-3} denoted by $Y_k(\sigma_{d-3})$, the Eq. (3.3.4) would have acquired a modification of the form $n^2 \to n^2 + k^2$, where $-k^2$ is the eigenvalue of the Laplace operator on Σ_{d-3}.

Introducing the inversion $z = (1 - \tanh\rho)/2$, we map $-\infty < \rho < +\infty$ to $1 > z > 0$, and obtain the asymptotic behavior for the radial dependence of the scalar field:

$$R(z) \quad \to \quad c_1 z^{\Delta_+} \left[1 + \mathcal{O}(z) \right] + c_2 z^{\Delta_-} \left[1 + \mathcal{O}(z) \right] \qquad \text{as } z \to 0, \tag{3.3.5}$$

and

$$R(z) \to d_1 (1-z)^{\Delta_+} \left[1 + \mathcal{O}(1-z) \right] + d_2 (1-z)^{\Delta_-} \left[1 + \mathcal{O}(1-z) \right] \qquad \text{as } z \to 1, \tag{3.3.6}$$

with

$$\Delta_\pm = \left(\frac{d-1}{4} \right) \pm \frac{1}{2} \sqrt{m^2 + \left(\frac{d-1}{2} \right)^2} , \tag{3.3.7}$$

$c_{1,2}$ and $d_{1,2}$ being integration constants.

Even though scalar fields on asymptotically AdS spacetimes can have negative m^2, we

will focus on the case $m^2 \geq 0$ (for a thorough analysis of the properties of a scalar field on the particular case of the wormhole with $\rho_0 = 0$ and the deformed Breitenlohner-Freedman bound, see (39)). Reflective boundary conditions require the field to vanish at infinity and therefore only the Δ_+ branch in (3.3.5) and (3.3.6) is allowed. Under these boundary conditions the equation (3.3.4) defines a Sturm-Liouville problem which can be manifestly seen by transforming the radial problem (3.3.4) into a Schrödinger-like equation.

In order to simplify the presentation, here after, let us fix the dimension to $d = 5$. Equation (3.3.4) can be written as

$$-\frac{d^2u}{d\bar{\rho}^2} + U(\bar{\rho})u = \omega^2 u \ , \tag{3.3.8}$$

where

$$u = R\cosh^{3/2}(\rho) \quad \text{and} \quad \rho = \rho_0 + \ln\left(\tan\left(\frac{\bar{\rho}}{2}\right)\right) \ . \tag{3.3.9}$$

The radial coordinate $\bar{\rho}$ works as a "tortoise"-like coordinate in the sense that in terms of $(t, \bar{\rho})$ the two-dimensional part of the metric (3.1.2) is manifestly conformally flat. The coordinate $\bar{\rho}$ connects both asymptotically AdS regions $0 < \bar{\rho} < \pi$. The effective Schrödinger potential takes the form

$$\begin{aligned} U(\bar{\rho}) = \frac{(4n^2-3)}{4}\left(\frac{\cos(\bar{\rho})\cosh(\rho_0) - \sinh(\rho_0)}{\cos(\bar{\rho}) - \coth(\rho_0)}\right)^2 - \left(2n^2-3\right)\left(\frac{\cos(\bar{\rho})\cosh(\rho_0) - \sinh(\rho_0)}{\cos(\bar{\rho})\,\mathrm{sech}(\rho_0) - \mathrm{csch}(\rho_0)}\right) \\ + \frac{\cosh^2(\rho_0)\,(4n^2-9)}{4} + \frac{(4m^2+15)}{4\sinh^2(\bar{\rho})} \, . \end{aligned} \tag{3.3.10}$$

This potential $U(\bar{\rho})$ (depicted in Figure 3.1), parametrically depends on the wormhole integration constant ρ_0, and for arbitrary values of the latter, the equation cannot be solved analytically. Even though we will solve the equation numerically to find the normal modes of the scalar probe on the wormhole, it is interesting to note that there are two particular values of ρ_0 for which the potential is shape invariant (40) and (3.3.8) can be solved analytically. Those values are $\rho_0 = 0$ and $\rho_0 \to +\infty$, and the corresponding potentials U are given by

$$U^{(0)}(\bar{\rho}) := \frac{15}{4}\frac{1}{\sin^2\bar{\rho}} + \frac{m^2}{\sin^2\bar{\rho}} - \frac{9}{4} + n^2 + \mathcal{O}\left(\rho_0\right) \ , \tag{3.3.11}$$

$$U^{(\infty)}(\bar{\rho}) := -\frac{1}{4}\frac{6\cos\bar{\rho} - 4m^2 - 9}{\sin^2\bar{\rho}} + \mathcal{O}\left(e^{-2\rho_0}\right) \ . \tag{3.3.12}$$

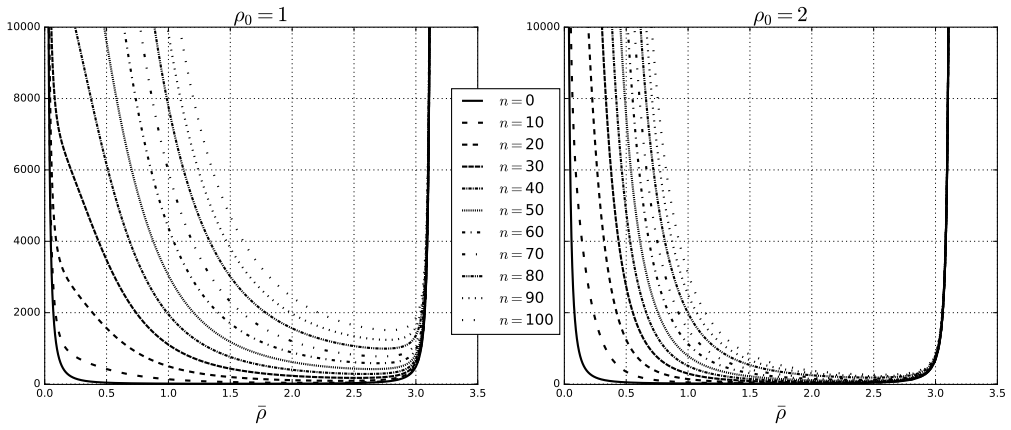

Figure 3.1: Effective potential for the radial dependence of the scalar probe, for different values of the parameters. As expected in the presence of a negative cosmological constant, the potential diverges at the boundaries $\bar{\rho} = 0, \pi$.

The leading term of $U^{(0)}$ leads to an effective quantum mechanical problem with a Rosen-Morse potential (45), which can be solved analytically and with energies and bound states given by

$$\omega^2_{(0),p} = \left(\frac{1}{2} + \sqrt{4+m^2} + p\right)^2 + n^2 - \frac{9}{4}\,, \tag{3.3.13}$$

$$u^{(0)}_p(\bar{\rho}) = A^{(0)}_p (\sin\bar{\rho})^{s+p} P_p^{(-s-p,-s-p)}(i\cot(\bar{\rho}))\ , \tag{3.3.14}$$

with $s = \sqrt{4+m^2} + 1/2$, $A^{(0)}_p$ an arbitrary integration constant that can be fixed by normalization, and $p = 0, 1, 2, 3, ...$ as the mode number. For the particular value $\rho_0 = 0$ the wormhole acquires a reflection symmetry with respect to the throat. ${P_a}^b$ are the corresponding Jacobi polynomials.

Remarkably, for $\rho_0 \to \infty$, the Schrödinger problem in (3.3.12) can also be integrated analytically since it corresponds to a Scarf potential (46), and leads to the following frequencies and eigenfunctions

$$\omega^2_{(\infty),p} = (A+p)^2\ , \tag{3.3.15}$$

$$u^{(\infty)}_p(\bar{\rho}) = A^{(\infty)}_p (1-\cos(\bar{\rho}))^{\frac{A-B}{2}} (\cos(\bar{\rho})+1)^{\frac{A+B}{2}} P_p^{\left(A-B-\frac{1}{2},A+B-\frac{1}{2}\right)}(\cos(\bar{\rho}))\ , \tag{3.3.16}$$

where the constant $A > B$ are given by

$$2A = 1 + \sqrt{5 + 2m^2 + 2\sqrt{(m^2+1)(m^2+4)}}\,, \tag{3.3.17}$$

$$6B = \left(5 + 2m^2 - 2\sqrt{(m^2+1)(m^2+4)}\right)\sqrt{5 + 2m^2 + 2\sqrt{(m^2+1)(m^2+4)}}, \tag{3.3.18}$$

where $A_p^{(\infty)}$ is an integration constant and $p = 0, 1, 2, ...,$ is again the mode number. It is worth to mention that in this case the frequencies $\omega_p^{(\infty)}$ lead to an equispaced, fully resonant spectrum. This result may be particularly relevant for obtaining the spectrum of the scalar field on the wormhole, for large ρ_0, by perturbative methods. The strict limit ρ_0 to infinity can be taken after suitable regularization of the geometry (37), leading to a wormhole that connects two different asymptotic regions. Since such wormhole is not asymptotically locally AdS we left its analysis for the section 3.6.

Here we are interested in the effects of a finite value of ρ_0 on the propagation of a minimally coupled scalar field. Therefore, we are obligated to integrate equation (3.3.8) numerically, with reflective boundary conditions at both infinities which can be achieved only for a countably infinity number of frequencies ω_p. This is done by using a variation of the so-called shooting method (see, for instance, (47)), which in our case consists in varying the value of ω in (3.3.8) and seeking those values which fulfill the boundary condition at $\bar{\rho} = \pi$. More specifically, the Schrödinger equation is recast as a first order ODE system, which is then integrated "from left to right", i.e. from $\bar{\rho} = 0$ to $\bar{\rho} = \pi$ for each value of ω. The integration is performed using the standard 4th order Runge-Kutta method (47), which thus determines the value of the solution at the right boundary, i.e. $u(\bar{\rho} = \pi, \omega)$. The later can be considered as a function of ω, for which the sought after values ω_p are zeros of, in virtue of the right boundary condition $u(\bar{\rho} = \pi, \omega_p)$. After a solution for ω_p is found, the value of p is determined by counting the number of nodes of the function $u(\bar{\rho}, \omega_p)$.

3.4 Spectra for the minimally coupled scalar probe

Since the problem for the normal modes with $\rho_0 \neq 0$ is a Sturm-Liouville problem, with potential fixed by the angular momentum of the field n, as well as ρ_0 and m^2, the eigenfunctions and eigenfrequencies will both be labeled by an integer p. In all the plots shown

below, we have included small black bars near $\rho_0 = 0$ and ρ_0 large, marking the analytic values for the frequencies obtained in those cases. In what follows we plot some of the numerically obtained spectra, which present interesting features as ρ_0 varies.

The frequencies of the fundamental mode ($p = 0$) are shown on the left panel of Figure 3.2, while the right panel shows a set of frequencies for the tenth overtone ($p = 10$). While the fundamental mode is a monotonic function of ρ_0, we observe that the excited modes have a maximum frequency for a critical value of ρ_0 and then decay to a given value. As expected, the frequencies increase with the angular momentum of the field, and consistently with the asymptotic expression for $U^{(\infty)}$ in Eq. (3.3.12), the frequencies merge regardless the value of n.

Figure 3.3 shows the fundamental and ten excited modes for the "s-wave" of the scalar ($n = 0$) on the left panel, while the frequencies for a spinning scalar probe with $n = 10$ have been plotted on the right-panel, both as a function of ρ_0. It is particularly interesting to notice that the "s-wave" fundamental and excited frequencies remain almost constant regardless the value of the integration constant ρ_0.

Finally, Figure 3.4 shows the fundamental and first overtones for different values of the angular momentum and the mass of the scalar. Even though the effective Schrödinger problem is one-dimensional, there are degeneracies due to the fact the effective potential depends on n, therefore different values of n lead to different one-dimensional Sturm-Liouville problems.

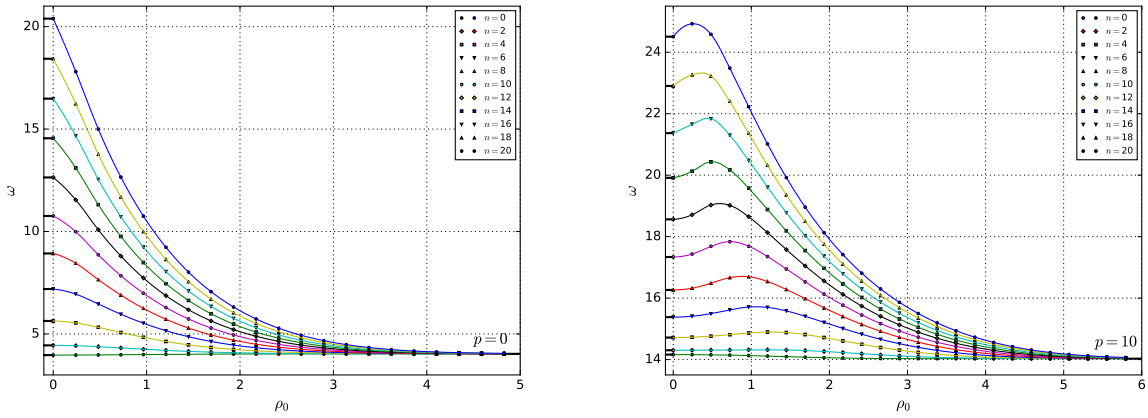

Figure 3.2: Spectra for the fundamental mode $p = 0$ (left-panel) and tenth overtone $p = 10$ (right-panel) as a function of ρ_0 for different even values of the angular momentum of the scalar probe $n = 0, 2, 4, ..., 10$, for $m^2 = 10$. The fundamental mode has a monotonic behavior with ρ_0 while excited frequencies present a maximum for a given critical value of ρ_0 which depends on the angular momentum of the field.

3.5 Scalars probes with nonminimal coupling

As shown in (39), for the case $\rho_0 = 0$ the equation for a scalar nonminimally coupled with the scalar curvature can also be solved in an analytic manner. This is remarkable since the Ricci scalar of the wormhole background is a nontrivial function of the radial coordinate ρ, therefore including a nonminimal coupling with the scalar curvature do not stand for a shift in the mass. Here, we explore the effect of a nonminimal coupling on the spectrum of the scalar for $\rho_0 \neq 0$, still within the context of dimension five. The equation for the scalar in this case is given by

$$\left(\Box - m^2 - \xi R\right) \Phi\left(x^\mu\right) = 0\,. \tag{3.5.1}$$

This scalar probe is invariant under local Weyl rescalings for $\xi = 3/16$. When ρ_0 vanishes, the equation for the radial dependence of the nonminimally coupled scalar can be obtained from that of the minimally coupled one by shifting the mass as well as the eigenvalues of the Laplace operator on the manifold $\Sigma_3 = S^1 \times H_2/\Gamma$. For nonvanishing ρ_0, one cannot rely on this shift, and one is forced to numerically find the spectrum of normal modes. Using the separation (3.3.3) and the change of variables (3.3.9), one leads to a Schrödinger-like equation of the form (3.3.8) with an intricate potential given by

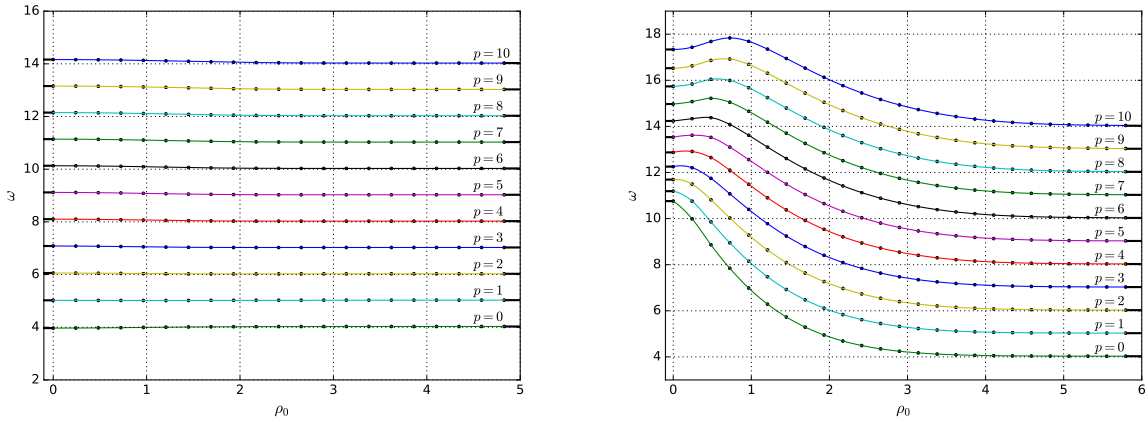

Figure 3.3: Spectra for vanishing angular momentum $n = 0$ (left-panel) and a spinning scalar probe with $n = 10$ (right-panel) as a function of ρ_0 for the fundamental mode and the first 10 excited states ($m^2 = 10$).

$$U_\xi(\bar{\rho}) = \frac{(4n^2-3)}{4}\left(\frac{\cos(\bar{\rho})\cosh(\rho_0)-\sinh(\rho_0)}{\cos(\bar{\rho})-\coth(\rho_0)}\right)^2 - \left(2n^2-3+6\xi\right)\left(\frac{\cos(\bar{\rho})\cosh(\rho_0)-\sinh(\rho_0)}{\cos(\bar{\rho})\,\mathrm{sech}(\rho_0)-\mathrm{csch}(\rho_0)}\right) + \frac{\cosh^2(\rho_0)\,(4n^2-9+24\xi)}{4} + \frac{(4m^2+15)}{4\sinh^2(\bar{\rho})}. \tag{3.5.2}$$

Even with the nonminimal coupling with the scalar curvature, in the extremal values $\rho_0 = 0$ and $\rho_0 \to \infty$ one also recovers shape invariant potentials, since

$$U_\xi^{(0)}(\bar{\rho}) = \left(\frac{15}{4}+m^2-20\xi\right)\frac{1}{\sin^2\bar{\rho}} + n^2 - \frac{9}{4} + 6\xi + O(\rho_0) \tag{3.5.3}$$

$$U_\xi^{(\infty)}(\bar{\rho}) = \frac{1}{4}\frac{6(4\xi-1)\cos\bar{\rho}+4m^2+9-56\xi}{\sin^2\bar{\rho}} + O\left(e^{-2\rho_0}\right), \tag{3.5.4}$$

corresponding to a Rosen-Morse potential and a Scarf potential, respectively.

It is interesting to note that for modes without angular momentum ($n = 0$) and $\xi = 3/8$ both potentials lead to a fully resonant, equispaced spectra, which might enhance the energy transfer between modes when nonlinearities are included (48), as it happens in AdS. Note that in a truly quantum-mechanical problem nor the Rosen-Morse, neither the Scarf potential lead to equispaced energies since in that case the eigenvalue is quadratic in the principal quantum number, and actually the harmonic oscillator is the unique potential with such property. Nevertheless, in our relativistic theory the eigenvalue is quadratic in the frequencies, therefore all the potentials which are quadratic in the principal quantum

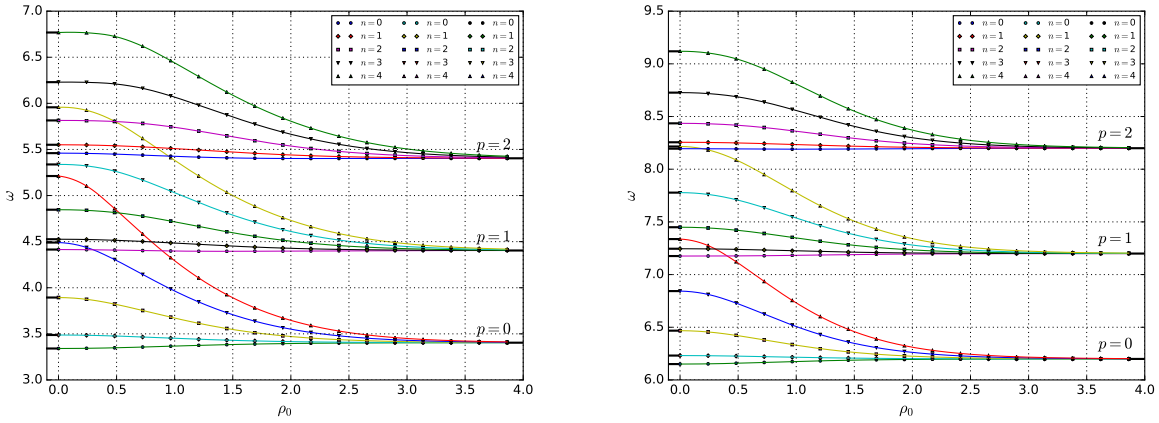

Figure 3.4: Fundamental and first two overtones for the scalar probe with $n = 0, 1, 2, 3, 4$, and $m^2 = 6$ (left-panel) and $m^2 = 30$ (right-panel). For a given value of ρ_0 the same frequency can be obtained for different modes since the effective potential depends explicitly on n.

number, may lead to a equispaced set of ω_n (see (49)).

The asymptotic behaviors for the function $R(z)$ with $z = (1 - \tanh(\rho))/2$ that defined the radial dependence of the field (3.3.3), is the same as that given in equations (3.3.5) and (3.3.6), replacing the,, conformal weights by

$$\Delta_{\pm}^{\xi} = 1 \pm \frac{1}{2}\sqrt{m^2 - 20\xi + 4}. \tag{3.5.5}$$

Regarding the asymptotic behavior one can define an effective mass $m^2_{\text{eff}} := m^2 - 20\xi$ and we will be focused in the region $m^2_{\text{eff}} \geq 0$, in which the reflective boundary conditions lead to a unique set of normal frequencies. Below, in Figure 3.5 and Figure 3.6, we present the spectra for different values of the parameters characterizing the potential, i.e., (ξ, ρ_0, m^2, n).

3.6 Scalar Probe Dynamics in a Regularized Wormhole Spacetime

Here we discuss some features of the scalar probe on the spacetime obtained after a suitable regularization in the limit $\rho_0 \to +\infty$. It is useful to return to Schwarzschild-like coordinates, that cover part of the wormhole spacetime (3.1.2). In such coordinates the

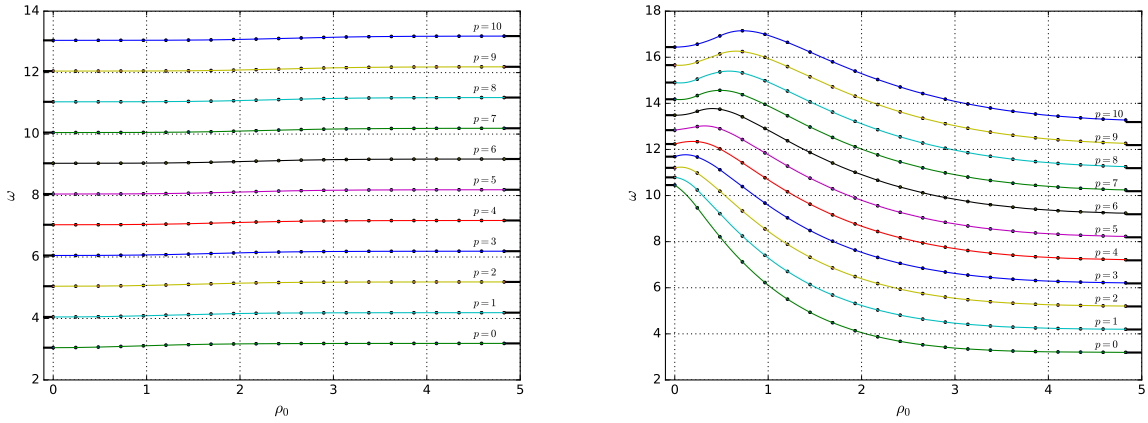

Figure 3.5: Fundamental and first overtones for the nonminimally coupled scalar probe without angular momentum ($n = 0$, left), and $n = 10$ (right), for $m^2 = 10$ and $\xi = 3/8$. The figure in the left smoothly connects two fully resonant spectra for $\rho_0 = 0$ and $\rho_0 \to \infty$.

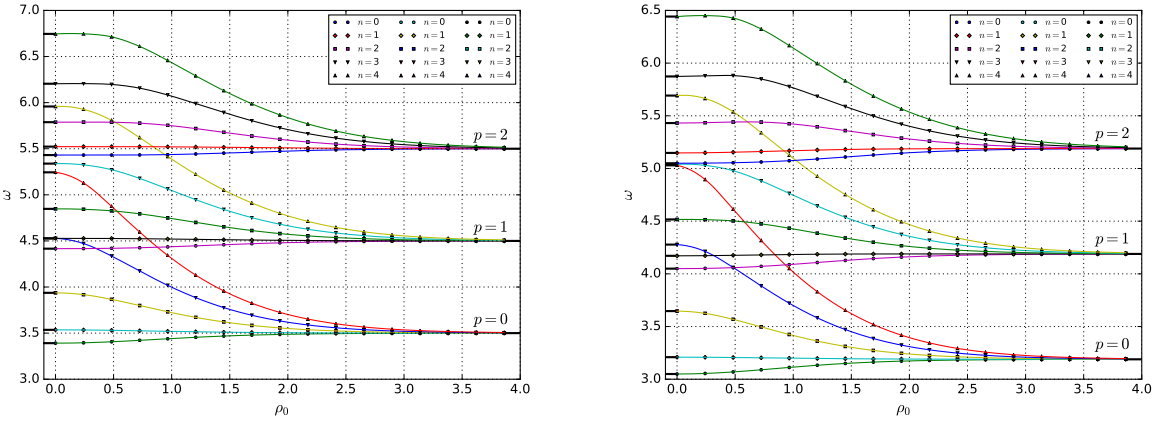

Figure 3.6: First three modes spectra for $\xi = 1/4$ (left) and $\xi = 3/8$ (right) for $m^2 = 10$ for $n = 0, 1, 2, 3, 4$.

metric reads (37)

$$ds^2 = -\left(\frac{r}{l^2} + a\sqrt{\frac{r^2}{l^2} - 1}\right)^2 d\bar{t}^2 + \left(\frac{r^2}{l^2} - 1\right)^{-1} dr^2 + r^2(d\varphi^2 + d\Sigma_2^2), \tag{3.6.1}$$

where $r = l\cosh(\rho)$, $t = \bar{t}/(l\cosh(\rho_0))$ and the integration constant ρ_0 relates to a by $\rho_0 := -\tanh^{-1}(a)$. Now we consider that $\rho_0 \to \infty$. In this case $a = -1$ and returning to the proper radial coordinate ρ one obtains

$$ds^2 = l^2\left[-e^{-2\rho}dt^2 + d\rho^2 + \cosh^2(\rho)(d\varphi^2 + d\Sigma_2^2)\right], \tag{3.6.2}$$

where $t = \bar{t}/l$. This solution also describes a wormhole geometry with a traversable throat located at $\rho = 0$. Note that this spacetime is asymptotically locally AdS only when $\rho \to -\infty$. Hereafter we set $l = 1$.

The radial equation for the nonminimally coupled scalar probe on this wormhole, for the ansatz $\Phi = e^{-i\omega t}e^{in\varphi}R(\rho)$ reduces to

$$\frac{d^2}{d\rho^2}R(\rho)-(1-3\tanh(\rho))\frac{d}{d\rho}R(\rho)+\left(e^{2\rho}\omega^2 - m^2 + (14 - 6\tanh(\rho))\xi - \frac{n^2}{\cosh^2(\rho)}\right)R(\rho) = 0. \tag{3.6.3}$$

The asymptotic behavior of the solution is given by

$$R(\rho) \overset{\rho\to-\infty}{\sim} A_1\ e^{(2-\sqrt{4+m^2-20\xi})\rho} + A_2\ e^{(2+\sqrt{4+m^2-20\xi})\rho} + \mathcal{O}(e^{2\rho}), \tag{3.6.4}$$

$$R(\rho) \overset{\rho\to\infty}{\sim} B_1\ e^{-3\rho/2-i\omega e^{\rho}} + B_2\ e^{-3\rho/2+i\omega e^{\rho}} + \mathcal{O}(e^{-\rho}). \tag{3.6.5}$$

As expected the behavior of the scalar when $\rho \to -\infty$ is a power law behavior on the areal coordinate $r \sim e^{\rho}$, typical of scalars on asymptotically AdS regions. While the behavior at the other non-AdS asymptotic region corresponds to that of an ingoing and outgoing wave. The equation can be solved analytically in terms on confluent Heun functions (50). The equation can be recast in a Schrödinger form by scaling the radial function and considering the ansatz $\Phi = e^{-i\omega t}e^{in\varphi}u(\rho)/\cosh^{3/2}(\rho)$ and using the new radial coordinate $\bar{\rho} = e^{\rho}$, with $\bar{\rho} \in (0, \infty)$, leading to

$$-\frac{d^2}{d\bar{\rho}^2}u(\bar{\rho}) + Uu(\bar{\rho}) = \omega^2 u(\bar{\rho}), \tag{3.6.6}$$

with the effective potential explicitly given in terms of the coordinate $\bar{\rho}$ by

$$U := \frac{m^2}{\bar{\rho}^2} - \frac{4(2\bar{\rho}^2+5)}{\bar{\rho}^2(\bar{\rho}^2+1)}\xi + \frac{4n^2}{(\bar{\rho}^2+1)^2} + \frac{3}{4}\frac{\bar{\rho}^4+2\bar{\rho}^2+5}{(\bar{\rho}^2+1)^2\bar{\rho}^2}. \tag{3.6.7}$$

Note that this potential depends explicitly on the angular momentum of the scalar n while $U_{\xi}^{(\infty)}$ defined in (3.5.4), does not. This confirms what we previously discuss in the paper regarding the fact that the exactly solvable potential obtained for the leading term of (3.5.4), has only to be thought as a tool to perturbatively obtain the frequencies for large ρ_0.

Note that here, at least on one side of the wormhole it is clear how to recognize ingoing

and outgoing modes. It would be interesting in this case to compute the transmission and reflection coefficients of the wormhole, along the lines of the computation of graybody factors in asymptotically AdS black holes (51).

3.7 A new wormhole solution of Einstein-Gauss-Bonnet and Lovelock theories

Before finishing, let us report on a new, wormhole solution of Einstein-Gauss-Bonnet or even Lovelock theories with a unique vacuum, provided (3.3.2), solve the corresponding field equations. The new wormhole geometry is given by

$$ds^2 = l^2 \left[-\cosh^2\rho\, dt^2 + d\rho^2 + \cosh^2(\rho-\rho_0)\, d\varphi^2 + \cosh^2\rho\, d\Sigma_2^2 \right], \tag{3.7.1}$$

that can be constructed from (3.3.2) via the double Wick rotation $t \to i\varphi$ and $\varphi \to it$. Notice that the double Wick rotation produces a different spacetime only when $\rho_0 \neq 0$, which is exactly the case we are considering in the present work. The geodesic equation on this background, freezing the dynamics along the coordinates of Σ_2, which must be of constant Ricci scalar curvature equal to -6, leads to

$$\dot{t} = \frac{E}{l^2\cosh^2\rho}\,, \quad \dot{\phi} = \frac{L}{l^2\cosh^2\rho - \rho_0}, \tag{3.7.2}$$

$$l^2\dot{\rho}^2 = -b + \frac{E^2}{l^2\cosh^2\rho} - \frac{L^2}{\cosh^2(\rho-\rho_0)}, \tag{3.7.3}$$

where L and E, are the angular momentum and the energy of the particle and $b = +1, 0, -1$ for timelike, null or spacelike geodesics, respectively. From the geodesic radial equation (3.7.3), one can see that the existence of a value of the radial coordinate $\rho = \rho_c$, for which the noncentrifugal (proportional to E^2) and the centrifugal (proportional to L^2) contributions balance, is nontrivial. In this case, the noncentrifugal contribution pushes toward the surface $\rho = 0$, while the centrifugal contribution pushes particles away from the surface $\rho = \rho_0$, in consequence, in the region $0 < \rho < \rho_0$, it is impossible to balance both contributions. A similar mechanism precludes the existence of orbits within the same region for the wormhole (3.3.2) (see (9)). On the other hand, the equation for a scalar field probe (3.3.1), (3.3.3), on the new geometry (3.7.1), leads to the following equation

for the radial dependence,

$$0 = \partial_\rho \left[\cosh(\rho-\rho_0)\cosh^3(\rho)\partial_\rho R(\rho)\right] + \\ + \cosh(\rho-\rho_0)\cosh^3(\rho)\left[-\frac{n^2}{\cosh^2(\rho-\rho_0)} + \frac{\omega^2}{\cosh^2(\rho-\rho_0)} - m^2 l^2\right] R(\rho), \qquad (3.7.4)$$

which exactly corresponds to (3.3.4) setting $d = 5$, $\omega \to in$ and $n \to i\omega$.

Before finishing this section, it is interesting to consider the energy content of the new wormhole geometry (3.7.1). For Einstein-Gauss-Bonnet, in five dimensions, at the Chern-Simons point, the regularized action principle of (52) leads, via Noether theorem, to a definition for the energy of an asymptotically locally AdS spacetime. The mass of the new wormhole (3.7.1) receives contributions from both boundaries $\rho \to \pm\infty$, which as for the wormhole (3.3.2) (see (9)), vanishes, since the contributions from both boundaries cancel each other, and in this case are given by

$$M^{\text{new}}_{\pm\infty} = \mp\frac{5\,\sigma_2}{8\pi G}\sinh\rho_0, \qquad (3.7.5)$$

where $\sigma_2 = 2\pi\text{Vol}(\Sigma_2)$. In this normalization, the contribution to the mass coming from each boundary on the original wormhole geometry (3.1.2) in dimension five reads $M^{\text{old}}_{\pm\infty} = \pm\frac{3\,\sigma_3}{8\pi G}\sinh\rho_0$. As mentioned above, in both cases the total mass vanishes.

In chapter 3 we have explored scalar probes on wormholes within Lovelock theories that exhibit a unique vacuum. The focus lies on constructing novel wormhole solutions in vacuum scenarios where coupling constants align all maximally symmetric solutions. This investigation extends previous work in Chern-Simons cases to arbitrary dimensions. A key element in this context is the integration constant ρ_0, which influences the energy content contribution from one boundary. The chapter delves into the impact of ρ_0 on the spectrum of massive, minimally or non-minimally coupled scalar probes under Dirichlet boundary conditions, resulting in a deformed Breitenlohner-Freedman bound sensitive to ρ_0. Detailed numerical results are presented for five-dimensional scenarios, including new wormhole geometries for the Einstein-Gauss-Bonnet theory with a unique vacuum. These geometries emerge through a double analytic continuation of previously known wormholes, introducing ρ_0 into the centrifugal terms for geodesic and scalar probes equations.

Transitioning from the detailed analysis of wormholes, Chapter 4 focuses on the study of (quasi)normal modes of de Sitter black holes and solitons within New Massive Grav-

ity (NMG). This theory, proposed by Bergshoeff, Hohm, and Townsend, expands three-dimensional gravity by incorporating a squared curvature scalar and Ricci tensor term. The chapter begins with an overview of the NMG theory and progresses to examine the exact quasinormal modes (QNMs) of scalar perturbations in black hole spacetimes and the normal modes (NMs) in asymptotically de Sitter solitons. The study of QNMs, which dates back around 50 years, reveals that black holes exhibit resonant waves that decay exponentially, providing insights into the late-stage dynamics of perturbations. The chapter also discusses the significance of QNMs in asymptotically de Sitter spacetimes, highlighting their astrophysical relevance due to the positive cosmological constant suggested by cosmological observations.

In summary, Chapter 3 lays the groundwork by investigating the scalar probe dynamics and wormhole geometries in Lovelock theories, setting the stage for Chapter 4, which transitions to the examination of quasinormal modes in black holes and solitons within the framework of New Massive Gravity. Both chapters contribute to a deeper understanding of gravitational theories and their implications for spacetime structures and perturbations.

Chapter 4

(Quasi)normal modes of de Sitter black holes and solitons in New Massive Gravity

The beginning of the study of quasinormal modes dates back to around 50 years ago (53). It was Vishveshwara who discovered that the majority of the waves coming from a black hole are resonant waves that decay exponentially. This means that a black hole loses energy when it has a perturbed field that decays over time. Although the quasinormal modes are an insufficient tool to understand the complete dynamics of a black hole, the study of them can give us valuable information about part of the dynamics of the gravitational system. For example, of the late stage of the disturbance.

On the other hand, the study of asymptotically de Sitter black holes, which have an event horizon and a cosmological horizon, may play an important role in astrophysics, since cosmological observations suggest the existence of a positive cosmological constant (54). Quasinormal modes in asymptotically de Sitter spacetimes were first studied by Moss et al. (55; 56), and from there, various methods were applied to asymptotically de Sitter gravitational systems in different dimensions (see e.g. (57; 58; 59; 60)).

The study of three-dimensional gravitational models has aroused strong interest in recent years. For example, the Topologically Massive Gravity (TMG) (61) which generalizes General Relativity by adding a gravitational Chern-Simons term to the theory. Bergshoeff, Hohm, and Townsend (BHT) introduced in 2009 the so-called New Massive Gravity (NMG) (62), which corresponds to the standard action of Einstein-Hilbert plus

a term that combines the squared curvature scalar and the squared Ricci tensor. New Massive Gravity supports various gravitational objects as solutions to the field equation such as dS and AdS black holes, dS, and AdS gravitational solitons, kinks, and wormholes (63), warped AdS black holes (64), asymptotically Lifshitz black holes (65), AdS waves (66; 67), among many others (68; 69; 70; 71; 72).

The main objective of this chapter is to study scalar field perturbations over asymptotically de Sitter three-dimensional black hole spacetime and gravitational solitons in NMG, calculate the (quasi)normal modes, and study their stability under scalar field perturbation. This work has been done in various contexts, for example in three-dimensional spacetime, the QNMs of the BTZ black hole (35) were studied in (73; 7; 74), the QNMs for scalar field perturbations in a new type black holes in NMG were studied in (75; 76) and the QNMs for fermion perturbations of some black holes in NMG were studied in (77).

In Section 4.1 we introduce a short review of the hairy black hole solution of massive $3D$ gravity. In Section 4.2 we analytically calculate the exact QNMs of scalar perturbations for the hairy black hole. In Section 4.3 we consider the asymptotically dS_3 soliton and calculate the normal modes (NMs) exactly.

4.1 New Massive Gravity

We consider the three-dimensional, parity-even massive gravity theory known as New Massive Gravity (NMG) (62). The action for NMG is given by

$$S = \frac{1}{16\pi G}\int d^3x\sqrt{-g}\left[R - 2\lambda - \frac{1}{m^2}K\right], \tag{4.1.1}$$

where

$$K := R_{\mu\nu}R^{\mu\nu} - \frac{3}{4}R^2. \tag{4.1.2}$$

The field equations are then of fourth order and read

$$G_{\mu\nu} + \lambda g_{\mu\nu} - \frac{1}{2m^2}K_{\mu\nu} = 0, \tag{4.1.3}$$

where

$$K_{\mu\nu} := 2\nabla^2 R_{\mu\nu} - \frac{1}{2}\left(\nabla_\mu\nabla_\nu R + g_{\mu\nu}\nabla^2 R\right) - 8R_{\mu\rho}R^{\rho}{}_{\nu} + \frac{9}{2}RR_{\mu\nu} + g_{\mu\nu}\left[3R^{\alpha\beta}R_{\alpha\beta} - \frac{13}{8}R^2\right]. \tag{4.1.4}$$

Generically, the theory admits solutions of constant curvature with two different curvatures, determined by

$$\Lambda_\pm = 2m\left(m \pm \sqrt{m^2 - \lambda}\right). \tag{4.1.5}$$

The field equations of NMG, at the special case $m^2 = \lambda$, admit the following exact, Euclidean solution (63)

$$ds^2 = \left(-\Lambda r^2 + br - \mu\right) d\psi^2 + \frac{dr^2}{-\Lambda r^2 + br - \mu} + r^2 d\varphi^2, \tag{4.1.6}$$

where b and μ are integration constants and $\Lambda := 2\lambda$. In this work, we will concentrate on the case with a positive cosmological constant. Therefore it is useful to define the above constant as $\Lambda := 1/\ell^2$. The metric of the static asymptotically de Sitter hairy black hole is given by

$$ds^2 = -\left(-\frac{r^2}{\ell^2} + br - \mu\right) dt^2 + \frac{dr^2}{-\frac{r^2}{\ell^2} + br - \mu} + r^2 d\varphi^2, \tag{4.1.7}$$

where $-\infty < t < \infty$, $0 \leq \varphi \leq 2\pi$. In terms of the corresponding roots, $r_{++} > r_+$, the metric reads

$$ds^2 = -\frac{1}{\ell^2}\left(r - r_+\right)\left(r_{++} - r\right) dt^2 + \frac{\ell^2 dr^2}{\left(r - r_+\right)\left(r_{++} - r\right)} + r^2 d\varphi^2, \tag{4.1.8}$$

where the gravitational hair and mass parameters are respectively given by

$$b = \frac{1}{\ell^2}\left(r_+ + r_{++}\right) > 0, \tag{4.1.9}$$

$$\mu = \frac{r_+ r_{++}}{\ell^2} > 0, \tag{4.1.10}$$

and possess a spatial singularity at $r = 0$ with the integration constants r_+ and r_{++} that are interpreted as event horizon and cosmological horizon respectively. The Ricci scalar for its geometry is given that

$$R = \frac{6}{\ell^2} - \frac{2b}{r}. \tag{4.1.11}$$

Note that global dS_3 spacetime is recovered for $b = 0$, and $\mu = -1$. The causal structure

of this spacetime corresponds to that of Schwarzschild de Sitter (see (63)).

In addition to the previous solution, NMG also admits a hairy dS_3 soliton (63). The gravitational soliton metric is related to the hairy black hole (4.1.8) through a double Wick rotation and reads

$$ds^2 = -\left((r_{++}+r_+)+(r_+-r_{++})\cos^2\theta\right)dt^2+\ell^2\left[d\theta^2+\sin^2\theta d\phi^2\right], \tag{4.1.12}$$

and the range of the coordinates is given by $-\infty < t < +\infty$, $0 \leq \phi \leq 2\pi$ and $0 \leq \theta \leq \pi$. In this case, the integration constants r_+ and r_{++} are no longer interpreted as horizons.

After a suitable rescaling of timelike coordinate, the metric turns out to depend on a single integration constant and reduces to

$$ds^2 = -\left(a+\cos\theta\right)^2 dt^2+\ell^2\left[d\theta^2+\sin^2\theta d\phi^2\right], \tag{4.1.13}$$

where $|a| > 1$, in order to avoid a potential curvature singularity. The Ricci scalar for (4.1.13) geometry is given that

$$R = \frac{1}{\ell^2}\frac{2a+3\cos\theta}{a+\cos\theta}. \tag{4.1.14}$$

Both the hairy black hole and the dS_3 soliton are conformally flat, so we will focus on the dynamics of a conformally coupled scalar field, which corresponds to the following field equation

$$\left(\Box-\frac{1}{8}R\right)\Phi = 0. \tag{4.1.15}$$

4.2 Black hole

The dynamics of a conformally coupled scalar probe on the hairy dS_3 black hole geometry is determined by the (4.1.8) metric.

Using the separation ansatz

$$\Phi \sim e^{-i\omega t+in\phi}H(r), \tag{4.2.1}$$

if $\ell = 1$, we arrive at the differential equation

$$\begin{aligned}(r_{++}-r)(r-r_+)H''(r) - \frac{1}{r}\left(3r^2 - 2r(r_+ + r_{++}) + r_+ r_{++}\right)H'(r) \\ - \left(\frac{n^2}{r^2} + \frac{\omega^2}{(r-r_{++})(r-r_+)} - \frac{1}{4}\frac{3r - r_+ - r_{++}}{r}\right)H(r) &= 0. \end{aligned} \quad (4.2.2)$$

It is convenient to define a new coordinate x such that

$$r = (r_{++} - r_+)\,x + r_+, \quad (4.2.3)$$

which maps $r_+ < r < r_{++}$ to $0 < x < 1$. In this way, the previous equation takes the following form

$$\begin{aligned}x(x-1)H''(x) + \frac{3x^2(r_+ - r_{++}) - 2x(2r_+ - r_{++}) + r_+}{r_+ x - r_{++}x - r_{++}}H'(x) \\ + \left[\frac{n^2}{(r_+ x - r_{++}x - r_{++})^2} + \frac{\omega^2}{x(x-1)(r_{++}-r_+)^2}\right. \\ \left. + \frac{1}{4}\frac{3x(r_+ - r_{++}) - 2r_+ + r_{++}}{r_+ x - r_{++}x - r_{++}}\right]H(x) &= 0, \end{aligned} \quad (4.2.4)$$

and the solution can be written as

$$\begin{aligned}H(x) &= (x-1)^{-\frac{i\omega}{r_{++}-r_+}}\left[C_1 x^{-\frac{i\omega}{r_{++}-r_+}}\left((x-1)r_+ - x r_{++}\right)^{c-\frac{3}{2}}\right. \\ &\quad {}_2F_1\left(a, b, c, \frac{r_{++}x}{(r_{++}-r_+)x + r_+}\right) + C_2 \frac{x^{\frac{i\omega}{r_{++}-r_+}}}{\sqrt{(x-1)r_+ - x r_{++}}} \\ &\quad \left. {}_2F_1\left(1+a-c, 1+b-c, 2-c, \frac{r_{++}x}{(r_{++}-r_+)x + r_+}\right)\right], \end{aligned} \quad (4.2.5)$$

where ${}_2F_1$ is the hypergeometric function and we have defined the constants a, b and c as

$$a = \frac{1}{2} - \frac{2i\omega}{r_{++}-r_+} - \frac{in}{\sqrt{r_+ r_{++}}}, \quad (4.2.6)$$

$$b = \frac{1}{2} - \frac{2i\omega}{r_{++}-r_+} + \frac{in}{\sqrt{r_+ r_{++}}}, \quad (4.2.7)$$

$$c = 1 + \frac{2i\omega}{r_{++}-r_+}. \quad (4.2.8)$$

Near the event horizon, the above expression behaves as

$$H(x \to 0) = \hat{C}_1 x^{-\frac{i\omega}{r_{++}-r_+}} + \hat{C}_2 x^{\frac{i\omega}{r_{++}-r_+}}. \quad (4.2.9)$$

Now, we impose as a boundary condition that classically nothing can escape from the event horizon. Note that $r_{++}-r_{+}>0$, therefore, we must take $C_2=0$ in order to have only ingoing waves at the event horizon. Consequently, the solution (4.2.5) simplifies to

$$H\left(x\right)=C_1\left(\left(x-1\right)x\right)^{-\frac{i\omega}{r_{++}-r_{+}}}\left(\left(x-1\right)r_{+}-xr_{++}\right)^{c-\frac{3}{2}}{}_2F_1\left(a,b,c,\frac{r_{++}x}{\left(r_{++}-r_{+}\right)x+r_{+}}\right). \tag{4.2.10}$$

Now, we implement boundary conditions at the cosmological horizon $x\to 1$. In order to do this, we employ Kummer's relations (6), which allows us to write the solution (4.2.10) as

$$\begin{aligned} H\left(x\right) &= \tilde{C}_1 x^{-\frac{i\omega}{r_{++}-r_{+}}}\left(\left(x-1\right)r_{+}-xr_{++}\right)^{c-\frac{3}{2}}\left[\left(1-x\right)^{-\frac{i\omega}{r_{++}-r_{+}}}\frac{\Gamma\left(c\right)\Gamma\left(c-a-b\right)}{\Gamma\left(c-a\right)\Gamma\left(c-b\right)}\right. \\ &\times{}_2F_1\left(a,b,1-c,1-\frac{r_{++}x}{\left(r_{++}-r_{+}\right)x+r_{+}}\right) \\ &+\left(1-x\right)^{-\frac{i\omega}{r_{++}-r_{+}}}\left(1-\frac{r_{++}x}{\left(r_{++}-r_{+}\right)x+r_{+}}\right)^{\frac{2i\omega}{r_{++}-r_{+}}}\frac{\Gamma\left(c\right)\Gamma\left(a+b-c\right)}{\Gamma\left(a\right)\Gamma\left(b\right)} \\ &\left.\times{}_2F_1\left(c-a,c-b,1+c-a-b,1-\frac{r_{++}x}{\left(r_{++}-r_{+}\right)x+r_{+}}\right)\right]. \end{aligned} \tag{4.2.11}$$

In order to have only outgoing waves at the cosmological horizon, we must impose $a=-p$ or $b=-p$, where p is a semipositive integer. These conditions yield the following set of quasinormal frequencies

$$\omega=\pm\frac{1}{2}\frac{\left(r_{++}-r_{+}\right)n}{\sqrt{r_{++}r_{+}}}-\frac{1}{4}i\left(1+2p\right)\left(r_{++}-r_{+}\right). \tag{4.2.12}$$

Due to the fact that the imaginary part of the QNFs is negative, the asymptotically dS_3 hairy black holes turn out to be stable under the conformal scalar field perturbation. Besides, being linear in the mode number p, leads to an equispaced damping spectrum. The s-wave modes, $n=0$ are all located on the imaginary axis, and the imaginary part of the frequencies is always negative, confirming the stability of the propagation. Interestingly enough, these properties are reminiscent of the spectrum of conformal waves for the asymptotically AdS_3 BTZ black hole (7), namely

$$\omega_{\mathrm{BTZ}}=\pm n-2ir_{+}(p+1), \tag{4.2.13}$$

Notice that for BTZ which has a completely different asymptotic structure, the real

part of the frequency is independent of the mass $M_{\rm BTZ} = r_+^2$. This is not the case for the static hairy black hole, for which both the oscillation frequencies and the damping depend on the mass. Even more, the differential eigenvalue problem leading to (4.2.13) on BTZ is completely different from the one to (4.2.12), since on BTZ there is no cosmological horizon. Regardless of these differences, the spectra on both spectra have a similar form.

4.3 Gravitational soliton

In what follows, we will study the response of the conformal scalar probe on the hairy soliton (4.1.13). Let us consider again the separable ansatz

$$\Phi \sim e^{-i\omega t + in\phi} P(\theta), \tag{4.3.1}$$

and define the useful change of coordinate given by

$$\rho = 1 - \frac{1}{2}\frac{(1+a)(\cos\theta + 1)}{a + \cos\theta}, \tag{4.3.2}$$

which maps $0 < \theta < \pi$ to $0 < \rho < 1$. In this way, for $\ell = 1$, the equation for the conformal scalar probe leads to

$$\begin{aligned} -P''(\rho) - \frac{2\rho^2 - (1-a)(1-2\rho)}{\rho(1-a-2\rho)(1-\rho)} P'(\rho) & \\ \left(\frac{1}{4}\frac{n^2}{\rho^2(1-\rho)^2} + \frac{\omega^2}{\rho(1-a^2)(1-\rho)} - \frac{1}{4}\frac{(a+3)(a+1) - 4a\rho}{\rho(1-a-2\rho)(1-\rho)} \right) P(\rho) &= 0, \end{aligned} \tag{4.3.3}$$

and its solution can be written as

$$\begin{aligned} P(\rho) &= (1-\rho)^{\frac{n}{2}} \sqrt{1-a-2\rho} \left[D_1 \rho^{\frac{n}{2}} {}_2F_1(\alpha, \beta, \gamma, \rho) \right. \\ &\quad \left. + D_2 \rho^{-\frac{n}{2}} {}_2F_1(1+\alpha-\gamma, 1+\beta-\gamma, 2-\gamma, \rho) \right], \end{aligned} \tag{4.3.4}$$

where we have defined the constants α, β and γ as

$$\alpha = n + \frac{1}{2} - \frac{\omega}{\sqrt{a^2-1}}, \tag{4.3.5}$$

$$\beta = n + \frac{1}{2} + \frac{\omega}{\sqrt{a^2-1}}, \tag{4.3.6}$$

$$\gamma = 1 + n. \tag{4.3.7}$$

In the expansion around $\theta = 0$ ($\rho = 0$), the equation (4.3.4) behaves as

$$P(\rho \to 0) \;=\; \hat{D}_1 \rho^{\frac{n}{2}} + \hat{D}_2 \rho^{-\frac{n}{2}}. \tag{4.3.8}$$

Now, we impose as a boundary condition that at the north pole the solution must be regular, for this, we must take $D_2 = 0$. So, the solution simplifies to

$$P(\rho) = D_1 \left((1-\rho)\,\rho\right)^{\frac{n}{2}} \sqrt{2\rho + a - 1}\, {}_2F_1(\alpha, \beta, \gamma, \rho). \tag{4.3.9}$$

Now, we implement boundary conditions at the south pole $\theta = \pi$ ($\rho = 1$). In order to do this, we again employ Kummer's relations, which allows us to rewrite the solution (4.3.9) as

$$\begin{aligned} P(\rho) \;=\; & \rho^{\frac{n}{2}} \sqrt{2\rho + a - 1} \left[\tilde{D}_1 (1-\rho)^{\frac{n}{2}} \frac{\Gamma(\gamma)\,\Gamma(\gamma-\alpha-\beta)}{\Gamma(\gamma-\alpha)\,\Gamma(\gamma-\beta)} {}_2F_1(\alpha, \beta, \alpha+\beta+1-\gamma, 1-\rho) \right. \\ & \left. + \check{D}_1 (1-\rho)^{-\frac{n}{2}} \frac{\Gamma(\gamma)\,\Gamma(\alpha+\beta-\gamma)}{\Gamma(\alpha)\,\Gamma(\beta)} {}_2F_1(\gamma-\alpha, \gamma-\beta, 1+\gamma+\alpha+\beta, 1-\rho) \right]. \end{aligned} \tag{4.3.10}$$

In the limit $\rho \to 1$, the above expression becomes

$$P(\rho \to 1) \;=\; \tilde{D}_1 (1-\rho)^{\frac{n}{2}} \frac{\Gamma(\gamma)\,\Gamma(\gamma-\alpha-\beta)}{\Gamma(\gamma-\alpha)\,\Gamma(\gamma-\beta)} + \check{D}_1 (1-\rho)^{-\frac{n}{2}} \frac{\Gamma(\gamma)\,\Gamma(\alpha+\beta-\gamma)}{\Gamma(\alpha)\,\Gamma(\beta)}. \tag{4.3.11}$$

Consequently, to obtain a regular solution at the south pole, we must impose $\alpha = -p$ or $\beta = -p$, where p is a semi-positive integer. These conditions yield the following set of frequencies

$$\omega = \pm \frac{1}{2} (2p - 2n - 1) \sqrt{a^2 - 1}. \tag{4.3.12}$$

As we can see, according to the definition introduced above $|a| > 1$, in this case, we find real frequencies, i.e. with normal modes.

Remarkably for the conformal probe (4.1.13) we can understand the result (4.3.12) by considering the general separable ansatz, as follows

$$\Phi = e^{-i\omega t} Y(\theta, \phi), \tag{4.3.13}$$

and noting that it is possible to solve this equation provided

$$\nabla_{S^2} Y = \left(-\omega^2 + \frac{1}{4}\right) Y, \tag{4.3.14}$$

it is possible to find a relationship between the frequency expressed in (4.3.14) and the spherical harmonics. This is because the equation (4.3.14) corresponds to the one for the spherical harmonics on S^2 since here ∇_{S^2} denotes the Laplacian on the round 2-sphere. In consequence $-\omega^2 + 1/4 = -l\,(l+1)$, where $l \in \mathbb{N}_0$. Thus, the frequency is equispaced in this case, since $\omega = l + 1/2$. In the case of the normal modes for the soliton (4.3.12) if p is left fixed and n varies, the distance between consecutive frequencies is $\sqrt{a^2 - 1}$, The same thing happens if n is left fixed and p varies.

Chapter 4 delved into the analysis of (quasi)normal modes of de Sitter black holes and gravitational solitons within the framework of New Massive Gravity (NMG). We explored the mathematical underpinnings and physical implications of these modes, providing exact solutions for scalar perturbations in specific spacetimes. The primary focus was on the stability and dynamical properties of these solutions, revealing crucial insights into the behavior of black holes and solitons in de Sitter spaces.

In this chapter, we discussed the resonance phenomena associated with black holes, where perturbations decay over time, shedding light on the energy dissipation mechanisms in these exotic objects. The (quasi)normal modes serve as a fingerprint of the spacetime geometry, offering a powerful tool to probe the properties of black holes and solitons.

Transitioning from the static spacetimes explored in Chapter 4, we now turn our attention to the more complex and astrophysically relevant scenario of rotating black holes. Chapter 5 moves beyond static spacetimes to investigate the perturbative dynamics in the context of rotating black holes, specifically the Kerr black hole. Given that real astrophysical black holes are expected to possess angular momentum, understanding the perturbations in such rotating systems is of paramount importance.

Chapter 5 begins by introducing the challenges and methodologies associated with studying perturbed fields in the spacetime of rotating black holes. Unlike static black holes, rotating black holes, such as the Kerr black hole, exhibit axial symmetry, which necessitates a different approach for analyzing perturbations. We delve into the historical and theoretical development of techniques, such as the Teukolsky equation, which enable the separation of variables in the study of rotating black holes.

We will also explore the application of the Newman-Penrose formalism and the analysis of perturbations in Petrov type D spacetimes, which are instrumental in understanding the behavior of various fields, including gravitational, electromagnetic, scalar, and neutrino fields, in the vicinity of rotating black holes.

By expanding our study from static to rotating black holes, we aim to provide a comprehensive understanding of the perturbative dynamics across different classes of black holes, thereby enriching our knowledge of these fascinating and fundamental objects in the Universe.

Chapter 5

Beyond static spacetimes

Since stars rotate, black holes should have at least angular momentum. This is why studying different perturbed fields over the spacetime of rotating black holes is necessary and interesting, due to its astrophysical interest. However, the Regge and Wheeler method (78), useful for studying static black holes (79; 80; 81; 82; 83; 84), is not suitable for the rotating Kerr black hole. This among other features is a consequence of the fact that the Kerr metric is only axisymmetric while the Regge-Wheeler approach considers metric perturbations with spherical symmetry, which leads to a system of coupled differential equations in radial and angular coordinates.

In 1968 B. Carter (85) showed for the first time that the method of separation of variables can be applied to the Kerr black hole. Finally, S. A. Teukolsky in 1972 and 1973 (86; 87) managed to solve this problem using the Newman-Penrose formalism, thus finding a master equation, which we now call the Teukolsky equation, which is completely separable, for perturbations of scalar, electromagnetic, gravitational and neutrino fields.

In this chapter, we will study the behavior of a special case of a rotating black hole when we perturb gravitational, electromagnetic, scalar, and neutrino fields. For this, it is necessary to introduce the Newman-Penrose formalism and the Petrov type D spacetimes, which will allow us to obtain Teukolsky's master equation, which is a second order partial differential equation for perturbed fields, see section 5.1.

To put the Newman-Penrose formalism into practice, in section 5.2 we will study the case of the rotating Kerr black hole in four dimensions, for which we will present the corresponding Teukolsky master equation. For more details on this exposition of this formalism see (88; 89).

In sections 5.2, 5.3 and 5.4 we present the results of the application of the Newman-Penrose formalism and the subsequent study of the perturbed field equations for the Kerr-AdS black hole and the Black Spindle, both in four dimensions, focusing on the axisymmetric symmetry modes. Finally, in sections 5.5, 5.6 and 5.7 we study the Kerr-AdS black hole and the Black Spindle in higher dimensions in a similar way to that done in the 4-dimensional case.

5.1 Newman-Penrose formalism

A Newman-Penrose (NP) frame is defined by four complex null vector fields $e_a = \{l, n, m, \bar{m}\}$ (the bar denotes complex conjugation) obeying the normalization conditions $l \cdot n = -1$, $m \cdot \bar{m} = 1$, $\ell \cdot m = 0$ and the metric tensor is the following

$$\eta_{ab} = \eta^{ab} = \begin{pmatrix} 0 & 1 & 0 & 0 \\ 1 & 0 & 0 & 0 \\ 0 & 0 & 0 & -1 \\ 0 & 0 & -1 & 0 \end{pmatrix}. \tag{5.1.1}$$

From the basis vectors we define the NP spin connection $\gamma_{cab} = e_b{}^{\mu} e_c{}^{\nu} \nabla_{\mu} e_{a\nu}$ with $\gamma_{cab} = -\gamma_{acb}$, the associated NP spin coeficients defined in terms of γ_{cab}, for historical reasons, are defined as

$$\begin{aligned} \kappa &= -\gamma_{311}, & \rho &= -\gamma_{314}, & \epsilon &= \frac{1}{2}(\gamma_{431} - \gamma_{211}), \\ \sigma &= -\gamma_{313}, & \mu &= \gamma_{423}, & \gamma &= \frac{1}{2}(\gamma_{122} - \gamma_{342}), \\ \lambda &= \gamma_{424}, & \tau &= -\gamma_{312}, & \alpha &= \frac{1}{2}(\gamma_{124} - \gamma_{344}), \\ \nu &= \gamma_{422}, & \pi &= \gamma_{421}, & \beta &= \frac{1}{2}(\gamma_{433} - \gamma_{213}), \end{aligned} \tag{5.1.2}$$

and the NP directional derivative operators $D = l^{\mu}\partial_{\mu}$, $\Delta = n^{\mu}\partial_{\mu}$, $\delta = m^{\mu}\partial_{\mu}$, $\bar{\delta} = \bar{m}^{\mu}\partial_{\mu}$.

Finally five, complex Weyl scalars Ψ_i, $i = 1, \cdots, 5$ are defined (C_{abcd} are the Weyl tensor components in the NP null basis):

$$\begin{aligned} \Psi_0 &= C_{1313} = C_{abcd} l^a m^b l^c m^d, \\ \Psi_1 &= C_{1213} = C_{abcd} l^a n^b l^c m^d, \end{aligned}$$

$$\begin{aligned}\Psi_2 &= C_{1342} = C_{abcd} l^a m^b \bar{m}^c n^d, \\ \Psi_3 &= C_{1242} = C_{abcd} l^a n^b \bar{m}^c n^d, \\ \Psi_4 &= C_{2424} = C_{abcd} n^a \bar{m}^b n^c \bar{m}^d,\end{aligned} \tag{5.1.3}$$

with

$$\begin{aligned} &C_{1334} = C_{1231} = \Psi_1, && C_{1241} = C_{1443} = \Psi_1^*, \\ &C_{1212} = C_{3434} = -(\Psi_2 + \Psi_2^*), && C_{1234} = (\Psi_2 - \Psi_2^*), \\ &C_{2443} = -C_{1242} = \Psi_3, && C_{1232} = C_{2343} = -\Psi_3^*, \end{aligned} \tag{5.1.4}$$

and $C_{1314} = C_{2324} = C_{1332} = C_{1442} = 0$.

We are interested in studying the perturbations of the fields, so it is necessary to find the differential equation. The NP formalism allows us to obtain coupled second-order partial differential equations. However, these differential equations can be decoupled for very special spacetimes, called Petrov type D spacetimes. All type D metrics are such that they meet the following characteristics

$$\Psi_0^A = \Psi_1^A = \Psi_2^A = \Psi_3^A = \Psi_4^A = 0, \tag{5.1.5}$$

$$\kappa^A = \sigma^A = \nu^A = \lambda^A = 0, \tag{5.1.6}$$

where we have defined the expansions of the most relevant quantities in the form $l = l^A + l^B + \ldots$, $\Psi = \Psi^A + \Psi^B + \ldots$, $D = D^A + D^B + \ldots$, etc. And the A terms correspond to the background, the B terms correspond to small perturbations, etc.

Let us denote the perturbations of the complex Weyl scalars Ψ_i by $\delta\Psi_i$. The important quantities for our discussion are $\delta\Psi_0$ and $\delta\Psi_4$, that correspond to gravitational perturbations with spin ± 2.

For $s = 2$ the Teukolsky equation is given by

$$\begin{aligned} &\{(D - 3\epsilon + \bar{\epsilon} - 4\rho - \bar{\rho})(\Delta + \mu - 4\gamma) \\ &- (\delta + \bar{\pi} - \bar{\alpha} - 3\beta - 4\tau)\left(\bar{\delta} + \pi - 4\alpha\right) - 3\Psi_2\big\}\,\delta\Psi_0 \;=\; 0, \end{aligned} \tag{5.1.7}$$

and, for $s=-2$ the Teukolsky equation is the following

$$\begin{aligned}&\{(\Delta+3\gamma-\bar{\gamma}+4\mu+\bar{\mu})(D+4\epsilon-\rho)\\ &-\left(\bar{\delta}-\bar{\tau}+\bar{\beta}+3\alpha+4\pi\right)(\delta-\tau+4\beta)-3\Psi_2\}\,\delta\Psi_4 \;=\; 0.\end{aligned} \tag{5.1.8}$$

5.2 Kerr-AdS black hole

The Kerr-AdS solution in Boyer-Lindquist coordinates is given by

$$\begin{aligned}ds^2 \;=\; &-\frac{\Delta_a}{\Sigma_a}\left(dt-\frac{a\sin^2\theta}{\Xi}d\varphi\right)^2+\frac{\Sigma_a}{\Delta_a}dr^2+\frac{\Sigma_a}{S}d\theta^2\\ &+\frac{S\sin^2\theta}{\Sigma_a}\left[adt-\frac{(r^2+a^2)}{\Xi}d\varphi\right]^2,\end{aligned} \tag{5.2.1}$$

where

$$\begin{aligned}J \;&:=\; \frac{aM}{\Xi^2},\quad \Sigma_a:=r^2+a^2\cos^2\theta,\quad \Xi:=1-\frac{a^2}{\ell^2},\quad S:=1-\frac{a^2}{\ell^2}\cos^2\theta,\\ \Delta_a \;&:=\; \left(r^2+a^2\right)\left(1+\frac{r^2}{\ell^2}\right)-2Mr,\quad a<\ell.\end{aligned}$$

The covariant Newman-Penrose null tetrad for the Kerr-AdS geometry in Boyer-Lindquist coordinates can be chosen as (90)

$$\begin{aligned}l_\mu dx^\mu \;&=\; \Delta_a\left\{\frac{1}{2\Sigma_a}dt+\frac{1}{\Delta_a}dr-\frac{1}{2}\frac{a\sin^2\theta}{\Sigma_a\Xi}d\varphi\right\},\\ n_\mu dx^\mu \;&=\; \left\{dt-\frac{\Sigma_a}{\Delta_a}dr-\frac{a\sin^2\theta}{\Xi}d\varphi\right\},\\ m_\mu dx^\mu \;&=\; \frac{\sin\theta\,(r+ia\cos\theta)}{\sqrt{2S}}\left\{\frac{iaS}{\Sigma_a}dt+\frac{1}{\sin\theta}d\theta-\frac{iS\,(r^2+a^2)}{\Sigma_a\Xi}d\varphi\right\}.\end{aligned} \tag{5.2.2}$$

This metric is a Petrov type D spacetime since all Weyl scalars, except Ψ_2, vanish: $\Psi_0=\Psi_1=\Psi_3=\Psi_4=0$, $\Psi_2=-M\,(r-ia\cos\theta)^{-3}$ and $\kappa^A=\sigma^A=\nu^A=\lambda^A=0$ (91).

The Teukolsky equation for $s=\pm2,\pm1,\pm3/2,\pm1/2$ in a Kerr-AdS geometry is given by the following expression (92)

$$\left[\frac{\left(r^2+a^2\right)^2}{\Delta_a}-\frac{a^2\sin^2\theta}{S}\right]\partial_t^2\Psi^{(s)}+2a\left[\frac{\left(r^2+a^2\right)\left(r^2+\ell^2\right)}{\ell^2\Delta_a}-1\right]\partial_t\partial_\varphi\Psi^{(s)}$$

$$
\begin{aligned}
&+\left[\frac{a^2\left(r^2+\ell^2\right)^2}{\ell^4\Delta_a}-\frac{S}{\sin^2\theta}\right]\partial_\varphi^2\Psi^{(s)}-\Delta_a^{-s}\partial_r\left(\Delta_a^{s+1}\partial_r\Psi^{(s)}\right)\\
&-\frac{1}{\sin\theta}\partial_\theta\left(\sin\theta S\partial_\theta\Psi^{(s)}\right)+s\left[\frac{4r\Delta_a-\left(r^2+a^2\right)\partial_r\Delta_a}{\Delta_a}+i\frac{2a\Xi\cos\theta}{S}\right]\partial_t\Psi^{(s)}\\
&-\frac{s}{\ell^2}\left[\frac{a\left(r^2+\ell^2\right)\partial_r\Delta_a}{\Delta_a}-4ar+i\frac{2\ell^2\Xi\cos\theta}{\sin^2\theta}\right]\partial_\varphi\Psi^{(s)}+\left\{\left(16s^8-120s^6+273s^4\right)\frac{\Sigma_a}{18\ell^2}\right.\\
&\left.+s^2\left(\frac{\Xi}{\sin^2\theta}-\frac{\Xi}{S}-\frac{277r^2+205a^2\cos^2\theta}{18\ell^2}\right)-s\left(1+\frac{a^2}{\ell^2}+\frac{6r^2}{\ell^2}\right)\right\}\Psi^{(s)} \;=\; 0.
\end{aligned}
\tag{5.2.3}
$$

We can write this equation in Boyer-Lindquist coordinates if we do the change of coordinates[1] $\varphi=\hat{\varphi}+at/\ell^2$, this way the previous equation can be written as follows

$$
\begin{aligned}
&\left(\frac{\left(r^2+a^2\right)^2}{\Delta_a}-\frac{a^2\sin^2\theta}{S}\right)\partial_t^2\Psi^{(s)}+\Xi\left(\frac{2a\left(r^2+a^2\right)}{\Delta_a}+\frac{2a}{S}\right)\partial_t\partial_{\hat{\varphi}}\Psi^{(s)}\\
&+\Xi^2\left(\frac{a^2}{\Delta_a}-\frac{1}{\sin^2\theta S}\right)\partial_{\hat{\varphi}}^2\Psi^{(s)}+s\left[\frac{4r\Delta_a-\left(r^2+a^2\right)\partial_r\Delta_a}{\Delta_a}+i\frac{2a\Xi\cos\theta}{S}\right]\partial_t\Psi^{(s)}\\
&-\Delta_a^{-s}\partial_r\left(\Delta_a^{s+1}\partial_r\Psi^{(s)}\right)-\frac{1}{\sin\theta}\partial_\theta\left(\sin\theta S\partial_\theta\Psi^{(s)}\right)\\
&-s\Xi\left(\frac{a\partial_r\Delta_a}{\Delta_a}+2i\cos\theta\left(\frac{1}{\sin^2\theta}+\frac{a^2}{\ell^2 S}\right)\right)\partial_{\hat{\varphi}}\Psi^{(s)}+\left\{\left(16s^8-120s^6+273s^4\right)\frac{\Sigma_a}{18\ell^2}\right.\\
&\left.+s^2\left(\frac{\Xi}{\sin^2\theta}-\frac{\Xi}{S}-\frac{277r^2+205a^2\cos^2\theta}{18\ell^2}\right)-s\left(1+\frac{a^2}{\ell^2}+\frac{6r^2}{\ell^2}\right)\right\}\Psi^{(s)} \;=\; 0.
\end{aligned}
\tag{5.2.4}
$$

Introducing the separation constant k and the ansatz

$$
\Phi\sim e^{-i\omega t+in\hat{\varphi}}R\left(r\right)Y\left(\theta\right), \tag{5.2.5}
$$

the Teukolsky master equation separates. The radial equation is

$$
\begin{aligned}
&\Delta_a^{-s}\frac{d}{dr}\left(\Delta_a^{s+1}\frac{dR\left(r\right)}{dr}\right)+\left\{-k+\frac{\left(\omega\left(r^2+a^2\right)-a\Xi n\right)^2}{\Delta_a\left(r\right)}+s\frac{\Delta_a'}{\Delta_a}\left(ia\Xi n-i\left(r^2+a^2\right)\omega\right)\right.\\
&\left.-\frac{8}{9}\frac{r^2s^8}{\ell^2}+\frac{20}{3}\frac{r^2s^6}{\ell^2}-\frac{91}{6}\frac{r^2s^4}{\ell^2}+\frac{277}{18}\frac{s^2r^2}{\ell^2}+\left(6\frac{r^2}{\ell^2}+4i\omega r\right)s\right\}R\left(r\right) \;=\; 0,
\end{aligned}
\tag{5.2.6}
$$

[1] We also can do this change of coordinates in momentum space, i.e. $\hat{n}=n$, $\hat{\omega}=\omega+an/\ell^2$ and we get the same equations.

while the angular equation is given by

$$\begin{aligned}
&\frac{d}{d\mu}\left(D_a\frac{dY(\mu)}{d\mu}\right)+\left\{k-\frac{\left(a\omega\left(1-\mu^2\right)+\Xi n\right)^2}{D_a}\right.\\
&-\frac{s\Xi}{D_a}\left(2\mu a\left(1-\mu^2\right)\omega-D_a'n\right)-\frac{a^2\mu^2}{\ell^2}\left(\frac{8}{9}s^8-\frac{20}{3}s^6+\frac{91}{6}s^4\right)\\
&\left.+\frac{\mu^2}{D_a}\left(\frac{205}{18}\frac{a^4\mu^4}{\ell^4}-\frac{205}{18}\frac{a^4\mu^2}{\ell^4}-\frac{205}{18}\frac{a^2\mu^2}{\ell^2}-\frac{a^4}{\ell^4}+\frac{241}{18}\frac{a^2}{\ell^2}-1\right)s^2+\left(1+\frac{a^2}{\ell^2}\right)s\right\}Y(\mu) \;=\; 0,
\end{aligned} \tag{5.2.7}$$

where $D_a(\mu):=\left(1-\mu^2\right)\left(1-a^2\mu^2/\ell^2\right)$. These equations define a system of two ordinary differential equations that are coupled through the eigenvalues k and ω, which must be found by imposing suitable regularity and boundary conditions.

5.3 Black Spindle

If we define a new azimuthal coordinate $\psi=\varphi/\Xi$, and then take the limit $a\to\ell$ in (5.2.1), we obtain the following spacetime (93)

$$ds^2 \;=\; -\frac{\Delta}{\Sigma}\left(dt-\ell\sin^2\theta d\psi\right)^2+\frac{\Sigma}{\Delta}dr^2+\frac{\Sigma}{\sin^2\theta}d\theta^2+\frac{\sin^4\theta}{\Sigma}\left[dt-\left(r^2+\ell^2\right)d\psi\right]^2, \tag{5.3.1}$$

where

$$J:=M\ell,\quad \Sigma:=r^2+a^2\cos^2\theta,\quad \Delta:=\left(\ell+\frac{r^2}{\ell}\right)^2-2Mr.$$

We note that ψ is a non-compact coordinate which we now compactify $\psi\sim\psi+\delta$, where the parameter δ is dimensionless.

Similarly to the previous procedure, the covariant Newman-Penrose null tetrad for the Kerr-AdS (5.2.2), takes the following form

$$\begin{aligned}
l_\mu dx^\mu &= \Delta\left\{\frac{1}{2\Sigma}dt+\frac{1}{2\Delta}dr-\frac{1}{2}\frac{\ell\sin^2\theta}{\Sigma}d\psi\right\},\\
n_\mu dx^\mu &= \left\{dt-\frac{\Sigma}{\Delta}dr-\ell\sin^2\theta d\psi\right\},\\
m_\mu dx^\mu &= \frac{(r+i\ell\cos\theta)}{\sqrt{2}}\left\{\frac{i\ell\sin^2\theta}{\Sigma}dt+\frac{1}{\sin\theta}d\theta-\frac{i\sin^2\theta\left(r^2+\ell^2\right)}{\Sigma}d\psi\right\}.
\end{aligned} \tag{5.3.2}$$

This tetrad shapes the Black Spindle geometry (94). In its contravariant form, it can be

written as follows

$$\begin{aligned} l^{\mu}\partial_{\mu} &= \left\{-\frac{1}{2}\frac{\ell^2+r^2}{\Sigma}\partial_t+\frac{1}{2}\frac{\Delta}{\Sigma}\partial_r-\frac{1}{2}\frac{\ell}{\Sigma}\partial_{\psi}\right\}, \\ n^{\mu}\partial_{\mu} &= \left\{-\frac{\ell^2+r^2}{\Delta}\partial_t-\partial_r-\frac{\ell}{\Delta}\partial_{\psi}\right\}, \\ m^{\mu}\partial_{\mu} &= \left\{\frac{i\ell\left(r+i\ell\cos\theta\right)}{\sqrt{2}\Sigma}\partial_t+\frac{\sin\theta}{\sqrt{2}\left(r-i\ell\cos\theta\right)}\partial_{\theta}+\frac{i\left(r+i\ell\cos\theta\right)}{\sqrt{2}\sin^2\theta\Sigma}\partial_t\right\}. \end{aligned} \tag{5.3.3}$$

It is important to note that this metric maintains the geometric property being a Petrov type D spacetime in this singular limit, since all Weyl scalars, except Ψ_2, vanish: $\Psi_0=\Psi_1=\Psi_3=\Psi_4=0$ y $\Psi_2=-M\left(r-i\ell\cos\theta\right)^{-3}$.

Replacing the values of the scalars (5.1.2) and of Ψ_2 corresponding to the geometry of the Black Spindle in (5.1.7), the Teukolsky equation takes the following form

$$\begin{aligned} &\left(\frac{\left(r^2+\ell^2\right)^2}{\Delta}-\ell^2\right)\partial_t^2\Psi^{(s)}+\left(\frac{2\ell\left(r^2+\ell^2\right)}{\Delta}-\frac{2\ell}{\sin^2\theta}\right)\partial_t\partial_{\psi}\Psi^{(s)} \\ &\quad+\left(\frac{\ell^2}{\Delta}-\frac{1}{\sin^4\theta}\right)\partial_{\psi}^2\Psi^{(s)}+s\frac{4r\Delta-\left(r^2+\ell^2\right)\partial_r\Delta}{\Delta}\partial_t\Psi^{(s)} \\ &-\Delta^{-s}\partial_r\left(\Delta^{s+1}\partial_r\Psi^{(s)}\right)-\frac{1}{\sin\theta}\partial_{\theta}\left(\sin^3\theta\partial_{\theta}\Psi^{(s)}\right)-s\left(\frac{\ell\partial_r\Delta}{\Delta}+\frac{4i\cos\theta}{\sin^2\theta}\right)\partial_{\psi}\Psi^{(s)} \\ &+\left(\left(16s^8-120s^6+273s^4\right)\frac{\Sigma_a}{18\ell^2}-s^2\frac{277r^2+205\ell^2\cos^2\theta}{18\ell^2}-s\left(2+\frac{6r^2}{\ell^2}\right)\right)\Psi^{(s)} = 0. \end{aligned} \tag{5.3.4}$$

and the radial and angular equations are given by

$$\begin{aligned} &\Delta^{-s}\frac{d}{dr}\left(\Delta^{s+1}\frac{dR\left(r\right)}{dr}\right)+\left\{-b+\frac{\left(\omega\left(r^2+\ell^2\right)-\ell k\right)^2}{\Delta\left(r\right)}+s\frac{\Delta'}{\Delta}\left(i\ell k-i\left(r^2+\ell^2\right)\omega\right)\right. \\ &\left.-\frac{8}{9}\frac{r^2s^8}{\ell^2}+\frac{20}{3}\frac{r^2s^6}{\ell^2}-\frac{91}{6}\frac{r^2s^4}{\ell^2}+\frac{277}{18}\frac{s^2r^2}{\ell^2}+\left(6\frac{r^2}{\ell^2}+4i\omega r\right)s\right\}R\left(r\right) = 0, \end{aligned} \tag{5.3.5}$$

$$\begin{aligned} &\frac{d}{d\mu}\left(D\left(\mu\right)\frac{dY\left(\mu\right)}{d\mu}\right)+\left\{b-\frac{\left(\ell\omega\left(1-\mu^2\right)+k\right)^2}{D\left(\mu\right)}+s\frac{D'\left(\mu\right)}{D\left(\mu\right)}k\right. \\ &\left.-\mu^2\left(\frac{8}{9}s^8-\frac{20}{3}s^6+\frac{91}{6}s^4\right)+\frac{205}{18}\mu^2s^2+2s\right\}Y\left(\mu\right) = 0, \end{aligned} \tag{5.3.6}$$

where $D\left(\mu\right):=\left(1-\mu^2\right)^2$. It is useful to work with the coordinate $\mu=\cos\theta$ such that $-1\leq\mu\leq+1$.

We observe that the singular limit can also be taken at this point. Note that by taking the limit $a\to\ell$ in the radial (5.2.6) and angular equations (5.2.7) for the Kerr-AdS black hole it is

possible to obtain the equations previously described for the Black Spindle.

In (5.3.5) and (5.3.6), b is a separation constant, and the system of ODE's is to be solved as a differential eigenvalue problem, which allows connecting the boundary conditions for some particular values of b and ω.

5.4 Axisymmetric modes in Black Spindle

First let us analyze the axisymmetric modes for a massless scalar probe in the Black Spindle, for that, we make $k = 0$ and $s = 0$ in (5.3.5) and (5.3.6). Moreover, using the redefinition of the separability constant $b = \omega^2 - c^2 + 1$ and considering $\ell = 1$, the angular equation reduces to

$$D(\mu)\frac{d^2Y(\mu)}{d^2\mu} - 4\left(1-\mu^2\right)\mu\frac{dY(\mu)}{d\mu} + \left(1-c^2\right)Y(\mu) = 0. \tag{5.4.1}$$

The general solution of this equation is

$$Y(\mu) = \mathcal{C}_1(c+\mu)(\mu-1)^{\frac{1}{2}c-\frac{1}{2}}(\mu+1)^{-\frac{1}{2}c-\frac{1}{2}} + \mathcal{C}_2(c-\mu)(\mu-1)^{-\frac{1}{2}c-\frac{1}{2}}(\mu+1)^{\frac{1}{2}c-\frac{1}{2}}, \tag{5.4.2}$$

and shows that there are no values for the constant c that allow us to smoothly connect the regular behavior at $\mu \to +1$ and $\mu \to -1$, in consequence, there are no axisymmetric modes in the black spindle with a massless scalar probe. Notice that $\mathrm{Re}\left(\frac{1}{2}c - \frac{1}{2}\right) > 0$ is satisfied when $\mathrm{Re}(c) > 1$, and $\mathrm{Re}\left(-\frac{1}{2}c - \frac{1}{2}\right) > 0$ is satisfied when $\mathrm{Re}(c) < -1$. Then we would need to cancel both constants of integration.

In the specific case when $\mathrm{Re}(c) = \pm 1$ the solution for (5.4.1) is the following

$$Y(\mu) = \mathcal{A}_1 + \mathcal{A}_2\left(-\frac{1}{4}\ln\left(\frac{\mu+1}{\mu-1}\right) - \frac{\mu}{2\left(\mu^2-1\right)}\right), \tag{5.4.3}$$

where we need to consider $\mathcal{A}_2 = 0$ in order to have regularity at the boundaries, obtaining a constant solution for the angular function.

Focussing on the radial equation (5.3.6) with $s = 0$ and imaginary positive frequency $\omega = i\Omega$ ($\Omega > 0$) in the horizon r_+, we obtain that $Y(\mu)$ is regular at the boundaries and vanishes at the horizon and at infinity. In this case, at least one turning point at some finite r must satisfy $R''/R < 0$ in order for both behaviors to be smoothly connected. However the quotient

$$\frac{R''}{R} = \frac{\ell^4\Omega^2 r r_+\left(\ell^2 + r_+^2\right)^2}{(r-r_+)^2\left(\ell^4 - 2\ell^2 r r_+ - r^3 r_+ - r_+^2 r^2 - r_+^3 r\right)^2} \tag{5.4.4}$$

is always positive. Therefore, it is not possible to obtain axisymmetric modes that connect

smoothly, not even for $Y(\mu) = \text{const}$.

If we consider the equations for any spin (5.3.6) and we redefine $b = 8s^8/9 - 20s^6/3 - c^2 + 91s^4/6 - 205s^2/18 + \omega^2 - 2s + 1$ we have the same behavior. The solution of the angular equation for $s = \pm 1/2, \pm 1, \pm 3/2, \pm 2$ is given by

$$Y(\mu) = \mathcal{D}_1 (\mu - 1)^{\frac{1}{2}c - \frac{1}{2}} (\mu + 1)^{-\frac{1}{2}c - \frac{1}{2}} + \mathcal{D}_2 (\mu - 1)^{-\frac{1}{2}c - \frac{1}{2}} (\mu + 1)^{\frac{1}{2}c - \frac{1}{2}} . \tag{5.4.5}$$

Therefore, there are no values for constant c that allow us to smoothly connect the regular behavior at $\mu \to \pm 1$. Therefore there are no axisymmetric modes in the black spindle for any field.

It is known that the Kerr and Kerr anti-de Sitter black holes have stable axisymmetric modes for a scalar perturbation (95; 96). It is surprising that in the case of the black spindle, these modes do not exist since this black hole is from the same family of spacetimes.

Having found an exact solution for the perturbation of a scalar field on the black spindle in 4 dimensions, it is interesting to study the behavior of this geometry in higher dimensions.

5.5 Kerr AdS black holes in higher dimensions

The d-dimensional Kerr anti de-Sitter geometry with a single rotation parameter given by

$$\begin{aligned} ds^2 &= -\frac{\Delta_a}{\Sigma_a}\left(dt - \frac{a}{\Xi}\sin^2\theta d\varphi\right)^2 + \frac{\Sigma_a}{\Delta_a}dr^2 + \frac{\Sigma_a}{S}d\theta^2 \\ &\quad + \frac{S\sin^2\theta}{\Sigma_a}\left(adt - \frac{r^2 + a^2}{\Xi}d\varphi\right)^2 + r^2\cos^2\theta d\Omega_{d-4}^2, \end{aligned} \tag{5.5.1}$$

where $\Delta_a := \left(r^2 + a^2\right)\left(1 + \frac{r^2}{\ell^2}\right) - 2Mr^{5-d}$, $\Sigma_a = r^2 + a^2\cos^2\theta$, $S = 1 - \frac{a^2}{\ell^2}\cos^2\theta$, $\Xi = 1 - \frac{a^2}{\ell^2}$, and $d\Omega_d^2$ denotes the metric element on a d-dimensional sphere.

The equation for the scalar probe in this case

$$\Box\Phi = 0, \tag{5.5.2}$$

assuming the mode separation

$$\Phi = e^{-i\omega t}e^{im\phi}R(r)\,Y(\theta)\,W\left(y^i\right), \tag{5.5.3}$$

where the function $W\left(y^i\right)$ corresponds to the spherical harmonic for the unit $(d-4)$-sphere[2]

$$\nabla^2_{S^{d-4}} W = -\lambda W\left(y^i\right), \tag{5.5.4}$$

with $\lambda = l\left(l+d-5\right)$, $l \in \mathbb{N}_0$. Introducing the separation constant, c the radial and angular equations are given by the following

$$\begin{aligned}\left(\frac{\Delta_a}{r} + \frac{\left(\ell^2+r^2\right)\left(a^2+r^2\right)d - \left(r^4+3\left(a^2+\ell^2\right)r^2+5a^2\ell^2\right)}{\ell^2 r}\right)\frac{dR\left(r\right)}{dr} + \\ \Delta_a \frac{d^2R\left(r\right)}{dr^2} + \left(-\frac{a^2\Xi^2m^2}{\Delta_a} - \frac{2a\left(a^2+r^2\right)\Xi m\omega}{\Delta_a}\right. \\ \left. + \left(\frac{\left(\ell^2+r^2\right)^2}{\Delta_a} - \ell^2\right)\omega^2 - \frac{a^2\lambda}{r^2} - \frac{c}{\ell^2}\right)R\left(r\right) &= 0,\end{aligned} \tag{5.5.5}$$

$$\begin{aligned}-\frac{1}{\mu}\left(1-\mu^2\right)\left(d\mu^2-d+4\right)\frac{dY\left(\mu\right)}{d\mu} + \left(1-\mu^2\right)^2\frac{d^2Y\left(\mu\right)}{d\mu^2} \\ + \left(\frac{2\ell n\omega}{1-\mu^2} - \frac{n^2}{\left(1-\mu^2\right)^2} - \frac{\lambda}{\mu^2} + \frac{c}{\ell^2}\right)Y\left(\mu\right) &= 0.\end{aligned} \tag{5.5.6}$$

5.6 Black Spindle in higher dimensions

Analogously to the previous sections, we define the coordinate $\psi = \phi/\Xi$, and then we take the limit $a \to \ell$ in (5.5.1). In this way we obtain the d-dimensional black spindle geometry which is given by

$$\begin{aligned}ds^2 &= -\frac{\Delta}{\Sigma}\left(dt - \ell\sin^2\theta d\phi\right)^2 + \frac{\Sigma}{\Delta}dr^2 + \frac{\Sigma}{\sin^2\theta}d\theta^2 \\ &\quad + \frac{\sin^4\theta}{\Sigma}\left(\ell dt - \left(r^2+\ell^2\right)d\phi\right)^2 + r^2\cos^2\theta d\Omega^2_{d-4},\end{aligned} \tag{5.6.1}$$

where $\Delta = \left(\ell + \frac{r^2}{\ell}\right)^2 - 2Mr^{5-d}$, $\Sigma = r^2 + \ell^2\cos^2\theta$, and $d\Omega^2_{d-4}$ denotes the metric element on a $(d-4)$-dimensional sphere.

Considering the probe scalar (5.5.2) and introducing the separation constant, c the radial and angular equations are given by the following

$$\left(\frac{\Delta}{r} + \frac{\left(\ell^2+r^2\right)^2 d - \left(r^4+6\ell^2r^2+5\ell^4\right)}{r\ell^2}\right)\frac{dR\left(r\right)}{dr} + \Delta\frac{d^2R\left(r\right)}{dr^2}$$

[2]For harmonic tensors we have equation (2.19) of (97) which in the case of rank zero, scalar tensors, reduces to (5.5.4) for spherical harmonics on the sphere of arbitrary dimension.

$$+\left(\frac{n^2\ell^2}{\Delta}-\frac{2\ell\left(\ell^2+r^2\right)\omega n}{\Delta}+\left(\frac{\left(\ell^2+r^2\right)^2}{\Delta}-\ell^2\right)\omega^2-\frac{\ell^2\lambda}{r^2}-\frac{c}{\ell^2}\right)R\left(r\right) = 0, \quad (5.6.2)$$

$$-\frac{1}{\mu}\left(1-\mu^2\right)\left(d\mu^2-d+4\right)\frac{dY\left(\mu\right)}{d\mu}+\left(1-\mu^2\right)^2\frac{d^2Y\left(\mu\right)}{d\mu^2} + \left(\frac{2\ell n\omega}{1-\mu^2}-\frac{n^2}{\left(1-\mu^2\right)^2}-\frac{\lambda}{\mu^2}+\frac{c}{\ell^2}\right)Y\left(\mu\right) = 0. \quad (5.6.3)$$

5.7 Axisymmetric modes for higher dimensions

Now we assume axial symmetry from (5.6.3), that is, $n = 0$, we also introduce a new constant b that will allow us to redefine the constant of integration c, through the following equation:

$$c = -4b^2\ell^2-4b\ell^2+\ell^2\lambda. \quad (5.7.1)$$

Thus, the angular equation takes the following form

$$-\frac{1}{\mu}\left(1-\mu^2\right)\left(d\mu^2-d+4\right)\frac{dY\left(\mu\right)}{d\mu}+\left(1-\mu^2\right)^2\frac{d^2Y\left(\mu\right)}{d\mu^2} + \left(-4b^2-4b-\frac{\lambda\left(1-\mu^2\right)}{\mu^2}\right)Y\left(\mu\right) = 0. \quad (5.7.2)$$

This corresponds to a hypergeometric differential equation whose solution is given by

$$Y\left(\mu\right) = \left(1-\mu^2\right)^{-b-1}\Big(\mathcal{B}_1\mu^{\triangle_+}{}_2F_1\left(\alpha,\beta,\gamma;\mu^2\right) + \mathcal{B}_2\mu^{\triangle_-}{}_2F_1\left(1+\alpha-\gamma,1+\beta-\gamma,2-\gamma;\mu^2\right)\Big), \quad (5.7.3)$$

where

$$\triangle_\pm = \frac{5}{2}-\frac{d}{2}\pm\frac{1}{2}\sqrt{\left(d-5\right)^2+4\lambda} \quad (5.7.4)$$

$$\begin{aligned}\alpha &= -b-\frac{1}{4}+\frac{d}{4}+\frac{1}{4}\sqrt{\left(d-5\right)^2+4\lambda},\\ \beta &= -b+\frac{1}{4}-\frac{d}{4}+\frac{1}{4}\sqrt{\left(d-5\right)^2+4\lambda},\\ \gamma &= 1+\frac{1}{2}\sqrt{\left(d-5\right)^2+4\lambda}.\end{aligned} \quad (5.7.5)$$

and $\mathcal{B}_1$ and $\mathcal{B}_2$ are integration constant.

Imposing regularity at the equator ($\mu = 0$) in (5.7.3), we must take $\mathcal{B}_2 = 0$ and $\mathcal{B}_1 = 1$ for $d \geq 5$ to obtain a nontrivial solution. Using properties of hypergeometric functions (6) in the

second term in (5.7.3), the solution takes the following form

$$\begin{aligned} Y(\mu) &= \mu^{\triangle_+}\Big(\left(1-\mu^2\right)^{-b-1}\frac{\Gamma(\gamma)\,\Gamma(\gamma-\alpha-\beta)}{\Gamma(\gamma-\alpha)\,\Gamma(\gamma-\beta)} \\ &\quad \times {}_2F_1\left(\alpha,\beta,\alpha+\beta+1-\gamma;1-\mu^2\right)+\left(1-\mu^2\right)^{b}\frac{\Gamma(\gamma)\,\Gamma(\alpha+\beta-\gamma)}{\Gamma(\alpha)\,\Gamma(\beta)} \\ &\quad \times {}_2F_1\left(\gamma-\alpha,\gamma-\beta,1+\gamma-\alpha-\beta;1-\mu^2\right)\Big). \end{aligned} \tag{5.7.6}$$

Now we study the regularity at the poles. If $b<-1$ the first term is regular at the poles, but not the second term, we need to find the condition for b where the gamma functions of the denominator become infinite. We see that

$$b=n-\frac{1}{4}+\frac{d}{4}+\frac{1}{4}\sqrt{(d-5)^2+4\lambda}, \tag{5.7.7}$$

with n a positive integer, however for $d\geq 5$, b must be positive, which is inconsistent with the initial condition for b, the same happens with the other gamma that appears in the denominator of this term. Studying the second term, we see that if $b\geq 0$, it is regular at the poles. Studying the gamma functions of the denominator of the first term, we see that

$$b=m-\frac{5}{4}+\frac{d}{4}-\frac{1}{4}\sqrt{(d-5)^2+4\lambda}, \tag{5.7.8}$$

with m a positive integer, which again for $d\geq 5$, b must be negative, which is contradictory with the condition for b. The same happens with the other gamma function in the denominator of the first term. When $-1<b<0$ the exponents of $(1-\mu^2)$ in both terms of the solution become indeterminate. The cases $b=0$ and $b=-1$ must be analyzed separately. If $b=0$ or $b=-1$, the equation (5.7.2) takes the following form:

$$-\frac{1}{\mu}\left(1-\mu^2\right)\left(\mu^2 d-d+4\right)\frac{dY(\mu)}{d\mu}+\left(1-\mu^2\right)^2\frac{d^2Y(\mu)}{d\mu^2}+\frac{\lambda\left(1-\mu^2\right)}{\mu^2}Y(\mu)=0. \tag{5.7.9}$$

Its solution is

$$\begin{aligned} Y(\mu) &= \mathcal{C}_1\mu^{\triangle_+}{}_2F_1\left(\alpha,\beta,\gamma;\mu^2\right) \\ &\quad +\mathcal{C}_2\mu^{\triangle_-}{}_2F_1\left(1+\alpha-\gamma,1+\beta-\gamma,2-\gamma;\mu^2\right), \end{aligned} \tag{5.7.10}$$

where we have used the notation (5.7.5), for $b=-1$. For $\lambda=0$ and considering regularity in the boundaries we obtain a constant solution for the angular function.

This study has illuminated the complexities of perturbations in rotating black holes, particularly through the use of the Newman-Penrose formalism and the Teukolsky master equation.

By extending these methods to Kerr-AdS black holes and specifically addressing the unique characteristics of the black spindle, we have broadened the scope of understanding in both theoretical and astrophysical contexts. The distinct properties of the black spindle provide valuable information on the behavior of rotating black holes in various space-time geometries.

Chapter 6

Conclusions

In this thesis, we presented three original results regarding perturbations of static and rotating black holes, as well as solitons and wormholes. We started by studying perturbations of a scalar field probe on an asymptotically locally AdS wormhole in five dimensions. Then we studied the scalar perturbations for two three-dimensional dS_3 spacetimes, the static hairy black hole, and the hairy gravitational soliton, both being three-dimensional NMG solutions and also conformally flat. Finally, we focused on a special type of rotating black hole, called a black spindle, which corresponds to the limit $a \to \ell$ of the Kerr black hole. We studied the disturbances of various fields through the Teukolsky method and we focused on perturbations of scalar fields.

In chapter 3 we have embedded in Lovelock theory in arbitrary dimensions, the $d = 2n + 1$-dimensional, wormhole geometry originally constructed in (9). The selected theories in even dimension are characterized by possessing a unique, maximally symmetric AdS vacuum, and the geometry of the wormhole throat is restricted to fulfill a tensor (3.2.6) and a scalar (3.2.7) constraint, containing one curvature less than the original theory. We have also obtained the spectrum of normal modes for a scalar probe on the asymptotically locally AdS wormhole in dimension five, complementing the work of (39), where the case $\rho_0 = 0$ was considered, a case that can be solved in an analytic manner. Here we have shown that the particular case with $\rho_0 = 0$ leads to a problem for the radial dependence of the scalar probe of the Schrödinger type, in the well-known Rosen-Morse potential. Remarkably, we have shown that when $\rho_0 \to \infty$, the spectrum can be also obtained in an analytic manner and it does not depend on the angular momentum of the scalar. This exact result can be useful to obtain the spectrum on a wormhole with a large, finite ρ_0 by perturbation theory. As discussed in section 3.6 the exact limit $\rho_0 \to \infty$ can be taken after suitable regularizations leading to a geometry that also describes a wormhole. We left some of the details of such case to section 3.6, since only one of the asymptotic regions is locally AdS in that setup. It is important to mention that since the g_{tt} component of the

metric is not a constant, the wormhole is not ultrastatic. Even more, for $\rho_0 \neq 0$ the minimum of the g_{tt} component of the metric does not coincide with the throat.

In (33), the authors considered a scalar probe propagating on the so-called natural wormholes that can be constructed by smoothly matching spherically symmetric solutions of GR, coupled to a Born-Infeld electrodynamics. In the effective radial eigenvalue problem, they imposed reflective boundary condition at one of the asymptotic regions and ingoing boundary conditions at the throat, leading to complex quasinormal frequencies. In our case, we have defined our eigenvalue problem by ensuring that the field is nondivergent at both asymptotic regions, requiring reflective boundary conditions when $\rho \to \pm\infty$.

The frequencies of the scalar field are given with respect to the coordinate time t, which in our case coincides with the proper time of a static observer located at $\rho = \rho_0$. Note that such observer is a geodesic one. In an asymptotically flat spacetime, as for example in the Schwarzschild black hole, the frequencies are referred to an observer located at the asymptotic region, which is independent of the value of the black hole mass. Nevertheless, when a negative cosmological constant is included, as for example in the four-dimensional Schwarzschild-AdS black hole, in Schwarzschild-like coordinates, a time dependence of the form $e^{-i\omega t}$ in a scalar probe implies that the frequencies correspond to those measured by an observer located at $r = \left(2Ml^2\right)^{1/3}$. Note that such observer is nongeodesic, in contraposition to our geodesic observer measuring frequencies in the wormhole. From the holographic viewpoint this coordinate time is actually the time in the dual CFT.

We have also included a nonminimal coupling between the scalar probe and the scalar curvature, which allows, for some particular values, to connect two fully resonant, equispaced spectra. It is worth to mention here also that fully resonant, equispaced spectra play a central role in the turbulent energy transfer that leads to nonperturbative AdS instability, see, e.g., (98; 99; 100; 101; 102; 103). This interesting phenomenology has also been observed in other nonlinear models as gravitating scalars on a spherical cavity in 3+1 (104), on systems governed by the Gross-Pitaevskii equation (105), on conformal dynamics on the Einstein Universe (106) and on vortex precession in Bose-Einstein condensates (107).

Finally, we have also introduced a new family of wormhole geometries, that are obtained from the first set via a double Wick rotation. The propagation of a test particle on this new geometry, unveils a region where no geodesic, circular orbit exist, and the spectrum of a scalar field probe can also be obtained from the one on the seed geometries by a suitable Wick rotation in frequency/momentum domain.

It would be interesting to explore the sector with negative squared masses. Since there is

an asymptotically locally AdS asymptotic behavior, it is natural to expect the existence of an effective Breitenlohner-Freedman bound that may depend on ρ_0 and that would have to be obtained numerically. We expect to report on this problem in the future.

In chapter 4 we have studied the scalar perturbations for two three-dimensional dS_3 spacetimes, the static hairy black hole, and the hairy gravitational soliton, both being three-dimensional NMG solutions, and also are conformally flat. It is noteworthy that we were able to analytically solve the response of the scalar field in such a background, which exists at the point at which the vacuum degenerates.

The first result that we present is that of a conformally coupled massless scalar field on the solution of the hairy black hole. We have analytically found QNMs for this asymptotically dS_3 black hole. The imaginary part of QNMs is negative, so these black holes are stable under conformally coupled scalar field perturbations. Also, the imaginary part is linear in mode number, leading to an equispaced damping spectrum. Finally, all the s-waves ($n = 0$) in equation (4.2.12) are located in the imaginary axis and this is always negative, which confirms the stability of the propagation.

The second result corresponds to the analysis of a conformally coupled scalar field on the asymptotically dS_3 hairy soliton. We find purely real frequencies, that is, frequencies with normal modes. Therefore this soliton corresponds to a non-dissipative system when we study a perturbed scalar field over this spacetime.

In chapter 5 we have explored the dynamics and perturbations in non-static spacetimes, focusing particularly on rotating black holes and the application of the Newman-Penrose formalism. We began by discussing the limitations of traditional methods like the Regge-Wheeler approach for rotating Kerr black holes and highlighted the advancements made by B. Carter and S. A. Teukolsky in solving this complex problem through the separation of variables and the Newman-Penrose formalism.

The Newman-Penrose formalism proved to be instrumental in deriving the Teukolsky master equation, which is applicable to perturbations of scalar, electromagnetic, gravitational, and neutrino fields in Kerr black holes. We detailed the process of obtaining this equation and its implications for understanding the behavior of perturbed fields in such spacetimes.

Moreover, we extended our analysis to the Kerr-AdS black hole, demonstrating the adaptability of the Newman-Penrose formalism and the Teukolsky equation in various spacetime geometries. This extension opens up new possibilities for studying the stability and dynamics of black holes in anti-de Sitter space, which has significant implications for both theoretical and astrophysical research.

Conclusiones

En esta tesis, presentamos tres resultados originales relacionados con las perturbaciones de agujeros negros estáticos y rotantes, así como de solitones y agujeros de gusano. Comenzamos estudiando las perturbaciones un campo escalar de prueba en un agujero de gusano asintóticamente AdS local en cinco dimensiones. Luego, estudiamos las perturbaciones escalares para dos espaciotiempos dS_3 tridimensionales: el agujero negro estático con pelo y el solitón gravitacional con pelo, ambos siendo soluciones de NMG tridimensionales y también conformemente planos. Finalmente, nos enfocamos en un tipo especial de agujero negro rotante, llamado Black Spindle, que corresponde al límite $a \to \ell$ del agujero negro de Kerr. Estudiamos las perturbaciones de varios campos mediante el método de Teukolsky y nos centramos en las perturbaciones de campos escalares.

En el capítulo 3 hemos embebido en la teoría de Lovelock en dimensiones arbitrarias, la geometía de agujero de gusano en dimensón $d = 2n + 1$ originalmente construida en (9). Las teorías seleccionadas en dimensiones pares se caracterizan por poseer un vacío AdS único y maximalmente simétrico, y la geometría de la garganta del agujero de gusano debe cumplir una restricción tensorial (3.2.6) y una restricción escalar (3.2.7), conteniendo una curvatura menos que la teoría original. También hemos obtenido el espectro de modos normales para un campo escalar en el agujero de gusano asintótica localmente AdS en dimensión cinco, complementando el trabajo de (39), donde se consideró el caso $\rho_0 = 0$, un caso que puede resolverse de manera analítica. Aquí hemos demostrado que el caso particular con $\rho_0 = 0$ lleva a un problema para la dependencia radial del campo escalar del tipo Schrödinger, en el conocido potencial de Rosen-Morse. Es importante notar que hemos demostrado que cuando $\rho_0 \to \infty$, el espectro también puede obtenerse de manera analítica y no depende del momento angular del escalar. Este resultado exacto puede ser útil para obtener el espectro en un agujero de gusano con un ρ_0 grande pero finito mediante teoría de perturbaciones. Como se discute en la sección 3.6, el límite exacto $\rho_0 \to \infty$ puede tomarse después de regularizaciones adecuadas que conducen a una geometría que también describe un agujero de gusano. Dejamos algunos de los detalles de ese caso para la sección 3.6, ya que solo una de las regiones asintóticas es localmente AdS

en ese contexto. Es importante mencionar que dado que la componente g_{tt} de la métrica no es constante, el agujero de gusano no es ultrastático. Aún más, para $\rho_0 \neq 0$ el mínimo de la componente g_{tt} de la métrica no coincide con la garganta.

En (33), los autores consideraron un campo escalar propagándose en los llamados agujeros de gusano naturales que pueden construirse emparejando suavemente soluciones esféricamente simétricas de la Relatividad General, acopladas a una electrodinámica de Born-Infeld. En el problema de autovalores radial efectivo, impusieron una condición de frontera reflectante en una de las regiones asintóticas y condiciones de frontera entrantes en la garganta, lo que llevó a frecuencias de modos cuasinormales complejas. En nuestro caso, hemos definido nuestro problema de autovalores asegurando que el campo no sea divergente en ambas regiones asintóticas, requiriendo condiciones de frontera reflectantes cuando $\rho \to \pm\infty$.

Las frecuencias del campo escalar se dan con respecto al tiempo coordenado t, que en nuestro caso coincide con el tiempo propio de un observador estático ubicado en $\rho = \rho_0$. Cabe señalar que dicho observador es geodésico. En un espaciotiempo asintóticamente plano, como por ejemplo en el agujero negro de Schwarzschild, las frecuencias se refieren a un observador ubicado en la región asintótica, que es independiente del valor de la masa del agujero negro. Sin embargo, cuando se incluye una constante cosmológica negativa, como por ejemplo en el agujero negro Schwarzschild-AdS de cuatro dimensiones, en coordenadas tipo Schwarzschild, una dependencia temporal de la forma $e^{-i\omega t}$ en un campo escalar implica que las frecuencias corresponden a las medidas por un observador ubicado en $r = \left(2Ml^2\right)^{1/3}$. Cabe seãlar que dicho observador no es geodésico, en contraposición con nuestro observador geodésico que mide frecuencias en el agujero de gusano. Desde el punto de vista holográfico, este tiempo coordenado es en realidad el tiempo en la CFT dual.

También hemos incluido un acoplamiento no minimal entre el campo escalar y la curvatura escalar, lo que permite, para algunos valores particulares, conectar dos espectros totalmente resonantes y equiespaciados. Vale la pena mencionar aquí también que los espectros totalmente resonantes y equiespaciados juegan un papel central en la transferencia de energía turbulenta que conduce a la inestabilidad AdS no perturbativa, véase, por ejemplo, (98; 99; 100; 101; 102; 103). Esta interesante fenomenología también se ha observado en otros modelos no lineales como escalares gravitacionales en una cavidad esférica en $3 + 1$ (104), en sistemas gobernados por la ecuación de Gross-Pitaevskii (105), en dinámica conformal en el Universo de Einstein (106) y en la precesión de vórtices en condensados de Bose-Einstein (107).

Finalmente, también hemos introducido una nueva familia de geometrías de agujeros de gusano, que se obtienen del primer conjunto mediante una doble rotación de Wick. La propagación

de una partícula de prueba en esta nueva geometría revela una región donde no existen órbitas circulares geodésicas, y el espectro de un campo escalar de prueba también puede obtenerse a partir del de las geometrías semilla mediante una rotación de Wick adecuada en el dominio de frecuencia/momento.

Sería interesante explorar el sector con masas al cuadrado negativas. Dado que existe un comportamiento asintótico localmente AdS, es natural esperar la existencia de un límite efectivo de Breitenlohner-Freedman que puede depender de ρ_0 y que tendría que obtenerse numéricamente. Esperamos informar sobre este problema en el futuro.

En el capítulo 4 hemos estudiado las perturbaciones escalares para dos espaciotiempos tridimensionales dS_3: el agujero negro estático con pelo y el solitón gravitacional con pelo, ambos siendo soluciones de NMG tridimensionales y también conformemente planos. Cabe destacar que pudimos resolver analíticamente la respuesta del campo escalar en tal contexto, que existe en el punto en que el vacío se degenera.

El primer resultado que presentamos es el de un campo escalar sin masa acoplado conformemente en la solución del agujero negro con pelo. Hemos encontrado analíticamente modos cuasinormales (QNMs) para este agujero negro asintóticamente dS_3. La parte imaginaria de los modos cuasinormales es negativa, por lo que estos agujeros negros son estables bajo perturbaciones de campo escalar acoplado conformemente. Además, la parte imaginaria es lineal en el número de modo, lo que lleva a un espectro de amortiguación equiespaciado. Finalmente, todas las ondas s ($n = 0$) en la ecuación (4.2.12) están ubicadas en el eje imaginario y esto siempre es negativo, lo que confirma la estabilidad de la propagación.

El segundo resultado corresponde al análisis de un campo escalar acoplado conformemente en el solitón con pelo asintóticamente dS_3. Encontramos frecuencias puramente reales, es decir, frecuencias con modos normales. Por lo tanto, este solitón corresponde a un sistema no disipativo cuando estudiamos un campo escalar perturbado en este espaciotiempo.

En el capítulo 5 hemos explorado la dinámica y las perturbaciones en espaciotiempos no estáticos, enfocándonos particularmente en los agujeros negros rotantes y la aplicación del formalismo de Newman-Penrose. Comenzamos discutiendo las limitaciones de los métodos tradicionales como el enfoque de Regge-Wheeler para los agujeros negros de Kerr rotantes y destacamos los avances realizados por B. Carter y S. A. Teukolsky en la resolución de este complejo problema mediante la separación de variables y el formalismo de Newman-Penrose.

El formalismo de Newman-Penrose resultó ser fundamental para derivar la ecuación maestra de Teukolsky, que es aplicable a las perturbaciones de campos escalares, electromagnéticos, gravitacionales y de neutrinos en agujeros negros de Kerr. Detallamos el proceso de obtención de

esta ecuación y sus implicaciones para comprender el comportamiento de los campos perturbados en tales espaciotiempos.

Además, extendimos nuestro análisis al agujero negro de Kerr-AdS, demostrando la adaptabilidad del formalismo de Newman-Penrose y la ecuación de Teukolsky en varias geometrías de espaciotiempo. Esta extensión abre nuevas posibilidades para estudiar la estabilidad y la dinámica de los agujeros negros en el espacio anti-de Sitter, lo que tiene importantes implicaciones tanto para la investigación teórica como astrofísica.

Bibliography

[1] Ch. W. Misner, K. S.Thorne and J. A. Wheeler. *Gravitation*. Macmillan, 1973.

[2] V. P. Frolov and I. D. Novikov. *Black Hole Physics: Basic Concepts and New Developments*. Kluwer, 1998.

[3] N. Aghanim, et al. *Astron. Astrophys.*, 617:A48, 2018. doi:10.1051/0004-6361/201731489.

[4] J. Maldacena. *Int. J. Theor. Phys.*, 38:1113–1133, 1999. doi:10.1023/A:1026654312961.

[5] M. Banados, C. Teitelboim and J. Zanelli. *Phys. Rev. D*, 49:975, 1994. doi:10.1103/PhysRevD.49.975.

[6] M. Abramowitz and I. A. Stegun. *Handbook of mathematical functions with formulas, graphs, and mathematical tables*, volume 55. US Government printing office, 1968.

[7] V. Cardoso and J. Lemos. *Phys. Rev. D*, 63:124015, 2001. doi:10.1103/PhysRevD.63.124015.

[8] T.R. Govindarajan and V. Suneeta. *Class. and Quantum Gravity*, 18:265, 2001. doi:10.1088/0264-9381/18/2/306.

[9] G. Dotti, J. Oliva and R. Troncoso. *Phys. Rev. D*, 75:024002, 2007. doi:10.1103/PhysRevD.75.024002.

[10] M. Visser. Lorentzian wormholes. from einstein to hawking. *Woodbury*, 1995.

[11] F.S.N. Lobo. Time machines and traversable wormholes in modified theories of gravity. In *EPJ Web Conf.*, volume 58, page 01006, 2013. doi:10.1051/epjconf/20135801006.

[12] R. Hennigar P. Bueno, P. Cano and R. Mann. *J. High Energy Phys.*, 2018(10):1–70, 2018. doi:10.1007/JHEP10(2018)095.

[13] E. Ayon-Beato, F. Canfora and J. Zanelli. *Phys. Lett. B*, 752:201–205, 2016. doi:10.1016/j.physletb.2015.11.065.

[14] J. Maldacena, A. Milekhin and F. Popov. *Class. Quantum Gravity*, 40:155016, 2018. doi:10.1088/1361-6382/acde30.

[15] A. Anabalon and J. Oliva. *J. High Energy Phys.*, 2019:1–12, 2019. doi:10.1007/JHEP04(2019)106.

[16] A. Anabalón, B. de Wit and J. Oliva. *J. High Energy Phys.*, 2020:1–23, 2020. doi:10.1007/JHEP09(2020)109.

[17] H. Ellis. *J. Math. Phys.*, 14:104–118, 1973. doi:10.1063/1.1666161.

[18] M. Morris and K. Thorne. *Am J Phys*, 56:395–412, 1988. doi:10.1119/1.15620.

[19] M. Morris, K. Thorne and U. Yurtsever. *Phys. Rev. Lett.*, 61:1446, 1988. doi:10.1103/PhysRevLett.61.1446.

[20] G. Clement. *Int. J. Theor. Phys.*, 23:335–350, 1984. doi:10.1007/BF02114513.

[21] S. Kar, D. Sahdev and B. Bhawal. *Phys. Rev. D*, 49:853, 1994. doi:10.1103/PhysRevD.49.853.

[22] D. Mishra S. Kar, S. Minwalla and D. Sahdev. *Phys. Rev. D*, 51:1632, 1995. doi:10.1103/PhysRevD.51.1632.

[23] P. Taylor. *Phys. Rev. D*, 95:109904, 2017. doi:10.1103/PhysRevD.95.109904.

[24] A. Hebecker, T. Mikhail and P. Soler. *Front. astron. space sci.*, 5:35, 2018. doi:DOI:10.3389/fspas.2018.00035.

[25] P. Betzios, N. Gaddam and O. Papadoulaki. *Phys. Rev. D*, 97:126006, 2018. doi:10.1103/PhysRevD.97.126006.

[26] C. Jonas, G. Lavrelashvili and JL. Lehners. *Phys. Rev. D*, 109:086022, 2024. doi:10.1103/PhysRevD.109.086022.

[27] A. Anabalón, Á. Arboleya and A. Guarino. *Phys. Rev. D*, 109:106007, 2024. doi:10.1103/PhysRevD.109.106007.

[28] J. L. Blázquez-Salcedo, L. M. González-Romero, B. Kleihaus, J. Kunz F. S. Khoo, B. Azad and F. Navarro-Lérida. *Phys. Rev. D*, 109:084013, 2024. doi:10.1103/PhysRevD.109.084013.

[29] S. Alfaro, P. A. González, D. Olmos, E. Papantonopoulos and Y. Vásquez. *Phys. Rev. D*, 109:104009, 2024. doi:10.1103/PhysRevD.109.104009.

[30] P. Breitenlohner and D. Freedman. *Phys. Lett. B*, 115:197–201, 1982. doi:10.1016/0370-2693(82)90643-8.

[31] P. Breitenlohner and D. Freedman. *Ann. Phys.*, 144:249–281, 1982. doi:10.1016/0003-4916(82)90116-6.

[32] L. Mezincescu and PK. Townsend. *Ann. Phys.*, 160:406–419, 1985. doi:10.1016/0003-4916(85)90150-2.

[33] J.Y. Kim, C. Lee and M. Park. *Eur. Phys. J. C*, 78:1–15, 2018. doi:10.1140/epjc/s10052-018-6478-5.

[34] M. Hassaine and J. Zanelli. *Chern-Simons (super) gravity*, volume 2. World Scientific, Singapur, 2016.

[35] M. Banados, C. Teitelboim and J. Zanelli. *Phys. Rev. Lett.*, 69:1849, 1992. doi:10.1103/PhysRevLett.69.1849.

[36] C. Teitelboim M. Banados, M. Henneaux and J. Zanelli. *Phys. Rev. D*, 48:1506, 1993. doi:10.1103/PhysRevD.48.1506.

[37] G. Dotti, J. Oliva and R. Troncoso. *Phys. Rev. D*, 76:064038, 2007. doi:10.1103/PhysRevD.76.064038.

[38] M. Ali, F. Ruiz, C. Saint-Victor and J. F. Vazquez-Poritz. *Phys. Rev. D*, 80:046002, 2009. doi:10.1103/PhysRevD.80.046002.

[39] D. Correa, J. Oliva and R. Troncoso. *J. High Energy Phys.*, 2008:081, 2008. doi:10.1088/1126-6708/2008/08/081.

[40] F. Cooper, A. Khare and U. Sukhatme. *Phys. Rep.*, 251:267–385, 1995. doi:10.1016/0370-1573(94)00080-M.

[41] R. Zegers. *J. Math. Phys.*, 46, 2005. doi:10.1063/1.1960798.

[42] S. Ray. *Class. Quantum Gravity*, 32:195022, 2015. doi:10.1088/0264-9381/32/19/195022.

[43] A. Anabalón, F. Canfora, A. Giacomini and J. Oliva. *Phys. Rev.D*, 84:084015, 2011. doi:10.1103/PhysRevD.84.084015.

[44] J. Matulich and R. Troncoso. *J. High Energy Phys.*, 2011:1–17, 2011. doi:10.1007/JHEP10(2011)118.

[45] N. Rosen and P. M. Morse. *Phys. Rev.*, 42:210, 1932.

[46] F. L. Scarf. *Phys. Rev.*, 112:1137, 1958.

[47] Mark Newman. *Computational physics*. Createspace Seattle, 2013.

[48] A. Anabalon, J. Oliva and C. Quijada. *Phys. Rev. D*, 99:104022, 2019. doi:10.1103/PhysRevD.99.104022.

[49] O. Evnin, H. Demirchian and A. Nersessian. *Phys. Rev. D*, 97:025014, 2018. doi:10.1103/PhysRevD.97.025014.

[50] A. Ronveaux and F. M. Arscott. *Heun's differential equations*. Clarendon Press, December 1995.

[51] S. Fernando. *Gen. Relativ. Gravit.*, 37:461–481, 2005. doi:10.1007/s10714-005-0035-x.

[52] P. Mora, R. Olea, R. Troncoso and J. Zanelli. *J. High Energy Phys.*, 2004:036, 2004. doi:10.1088/1126-6708/2004/06/036.

[53] C. Vishveshwara. *Nature*, 227:936–938, 1970. doi:10.1038/227936a0.

[54] G. Perlmutter et al. *The Astrophysical Journal*, 517:565, 1999. doi:10.1086/307221.

[55] F. Mellor and I. Moss. *Phys. Rev. D*, 41:403, 1990. doi:10.1103/PhysRevD.41.403.

[56] I. Moss and J. Norman. *Class. Quantum Gravity*, 19:2323, 2002. doi:10.1088/0264-9381/19/8/319.

[57] V. Cardoso and J. Lemos. *Phys. Rev. D*, 67:084020, 2003. doi:10.1103/PhysRevD.67.084020.

[58] C. Molina. *Phys. Rev. D*, 68:064007, 2003. doi:10.1103/PhysRevD.68.064007.

[59] A. Maassen van den Brink. *Phys. Rev. D*, 68:047501, 2003. doi:10.1103/PhysRevD.68.047501.

[60] V. Suneeta. *Phys. Rev. D*, 68:024020, 2003. doi:10.1103/PhysRevD.68.024020.

[61] S. Deser, R. Jackiw and S. Templeton. *Phys. Rev. Lett*, 48:975, 1982. doi:10.1103/PhysRevLett.48.975.

[62] E. Bergshoeff, O. Hohm and P. Townsend. *Phys. Rev. Lett.*, 102:201301, 2009. doi:10.1103/PhysRevLett.102.201301.

[63] J. Oliva, D. Tempo and R. Troncoso. *J. High Energy Phys.*, 2009:011, 2009. doi:10.1088/1126-6708/2009/07/011.

[64] G. Clement. *Class Quantum Gravity*, 26:105015, 2009. doi:10.1088/0264-9381/26/10/105015.

[65] E. Ayon-Beato, A. Garbarz, G. Giribet and M. Hassaine. *Phys. Rev. D*, 80:104029, 2009. doi:10.1103/PhysRevD.80.104029.

[66] G. Clement. *Class Quantum Gravity*, 26:165002, 2009. doi:10.1088/0264-9381/26/16/165002.

[67] E. Ayon-Beato, G. Giribet and M. Hassaine. *J. High Energy Phys.*, 2009:029, 2009. doi:10.1088/1126-6708/2009/05/029.

[68] S. Deser. *Phys. Rev Lett.*, 103:101302, 2009. doi:10.1103/PhysRevLett.103.101302.

[69] W. Kim and E. J. Son. *Phys. Lett. B*, 678:107–111, 2009. doi:10.1016/j.physletb.2009.06.005.

[70] Y. Liu and Y. Sun. *Phys. Rev. D*, 79:126001, 2009. doi:10.1103/PhysRevD.79.126001.

[71] M. Nakasone and I. Oda. *Phys. Rev. D*, 79:104012, 2009. doi:10.1103/PhysRevD.79.104012.

[72] I. Oda. *J. High Energy Phys.*, 2009:064, 2009. doi:10.1088/1126-6708/2009/05/064.

[73] J. Chan and R. Mann. *Phys. Rev. D*, 55:7546, 1997. doi:10.1103/PhysRevD.55.7546.

[74] D. Birmingham, I. Sachs and S. Solodukhin. *Phys. Rev. Lett.*, 88:151301, 2002. doi:10.1103/PhysRevLett.88.151301.

[75] M. Chernicoff, G. Giribet, J. Oliva and R. Stuardo. *Phys. Rev. D*, 102:084017, 2020. doi:10.1103/PhysRevD.102.084017.

[76] Y. Kwon, S. Nam, J. Park and S. Yi. *Class. Quantum Gravity*, 28:145006, 2011. doi:10.1088/0264-9381/28/14/145006.

[77] P. Gonzalez and Y. Vasquez. *Eur Phys. J. C*, 74:1–9, 2014. doi:10.1140/epjc/s10052-014-2969-1.

[78] T. Regge and J. A. Wheeler. *Phys. Rev.*, 108:1063, 1957. doi:10.1103/PhysRev.108.1063.

[79] F. J. Zerilli. *Phys. Rev. D*, 9:860, 1974. doi:10.1103/PhysRevD.9.860.

[80] V. Moncrief. *Phys. Rev. D*, 9:2707, 1974. doi:10.1103/PhysRevD.9.2707.

[81] V. Moncrief. *Phys. Rev. D*, 10:1057, 1974. doi:10.1103/PhysRevD.10.1057.

[82] J. Bičák. *Gen. Relativ. Gravit.*, 3:331–349, 1972. doi:10.1007/BF00759172.

[83] J. Bičák. *Gen. Relat. Gravit.*, 12:195–204, 1980. doi:10.1007/BF00756232.

[84] J. Bičák. Perturbations of the reissner-nordstrom black hole. In Remo Ruffini, editor, *The Proceedings of the Second Marcel Grossmann Meeting on General Relativity*, page 277, 1982.

[85] B. Carter. *Commun. Math. Phys.*, 10:280–310, 1968. doi:10.1007/BF03399503.

[86] A. S. Teukolsky. *Phys. Rev. Lett.*, 29:1114, 1972. doi:10.1103/PhysRevLett.29.1114.

[87] S. A. Teukolsky. *Astrophys. J.*, 185:635–648, 1973. doi:10.1086/152444.

[88] V. Frolov and I. Novikov. *Black Hole Physics: Basic Concepts and New Developments*. Springer Science & Business Media, 2012.

[89] D. Bini, C. Cherubini, R. Jantzen and R. Ruffini. *Prog. Theor. Phys.*, 107:967–992, 2002. doi:10.1143/PTP.107.967.

[90] W. Kinnersley. *J. Math. Phys.*, 10:1195–1203, 1969. doi:10.1063/1.1664958.

[91] O. Dias and J. Santos. *J. High Energy Phys.*, 2013:156, 2013. doi:10.1007/JHEP10(2013)156.

[92] O. Dias, J. Santos M. and Stein. *J. High Energy Phys.*, 2012:182, 2012. doi:10.1007/JHEP10(2012)182.

[93] R. Hennigar, D. Kubiznak and R. Mann. *Phys. Rev. Lett.*, 115:031101, 2015. doi:10.1103/PhysRevLett.115.031101.

[94] J. F. Plebanski and M. Demianski. *Ann. Phys.*, 98:98–127, 1976. doi:10.1016/0003-4916(76)90240-2.

[95] P. Montero, L. Rezzolla and S. Yoshida. *Mon. Not. R. Astron. Soc.*, 354:1040–1052, 2004. doi:10.1111/j.1365-2966.2004.08265.x.

[96] N. Uchikata, S. Yoshida and T. Futamase. *Phys. Rev. D*, 80:084020, 2009. doi:10.1103/PhysRevD.80.084020.

[97] A. Higuchi. *J. Math. Phys.*, 28:1553, 1987. doi:10.1063/1.527513.

[98] P. Bizon and A. Rostworowski. *Phys. Rev. Lett.*, 107:031102, 2011. doi:10.1103/PhysRevLett.107.031102.

[99] O. Dias, G. Horowitz and J. Santos. *Class. Quantum Gravity*, 29:194002, 2012. doi:10.1088/0264-9381/29/19/194002.

[100] V. Balasubramanian, A. Buchel, S. Green, L. Lehner and S. Liebling. *Phys. Rev. Lett.*, 113:071601, 2014. doi:10.1103/PhysRevLett.113.071601.

[101] B. Craps, O. Evnin and J. Vanhoof. *J. High Energy Phys.*, 2014:1–31, 2014. doi:10.1007/JHEP10(2014)048.

[102] O. Evnin B. Craps and J. Vanhoof. *J. High Energy Phys.*, 2015:1–28, 2015. doi:10.1007/JHEP01(2015)108.

[103] P. Bizon, M. Maliborski and A. Rostworowski. *Phys. Rev. Lett.*, 115:081103, 2015. doi:10.1103/PhysRevLett.115.081103.

[104] M. Maliborski. *Phys. Rev. Lett.*, 109:221101, 2012. doi:10.1103/PhysRevLett.109.221101.

[105] A. Biasi, P. Bizon, B. Craps and O. Evnin. *Phys. Rev. E*, 98:032222, 2018. doi:10.1103/PhysRevE.98.032222.

[106] P. Bizon, B. Craps, O. Evnin, D. Hunik, V. Luyten and M. Maliborski. *Commun. Math. Phys.*, 353:1179–1199, 2017. doi:10.1007/s00220-017-2896-8.

[107] A. Biasi, P. Bizon, B. Craps and O. Evnin. *Phys. Rev. A*, 96:053615, 2017. doi:10.1103/PhysRevA.96.053615.